PBHs and Gravitational Waves

Antonio Riotto
University of Geneva

Plan of the talk

- PBHs in the LIGO/Virgo mass range and GWs from mergers
- PBHs in the light mass range and the stochastic background of GWs

In collaboration with V. De Luca, V. Desjacques, G. Franciolini, and P. Pani

Motivation

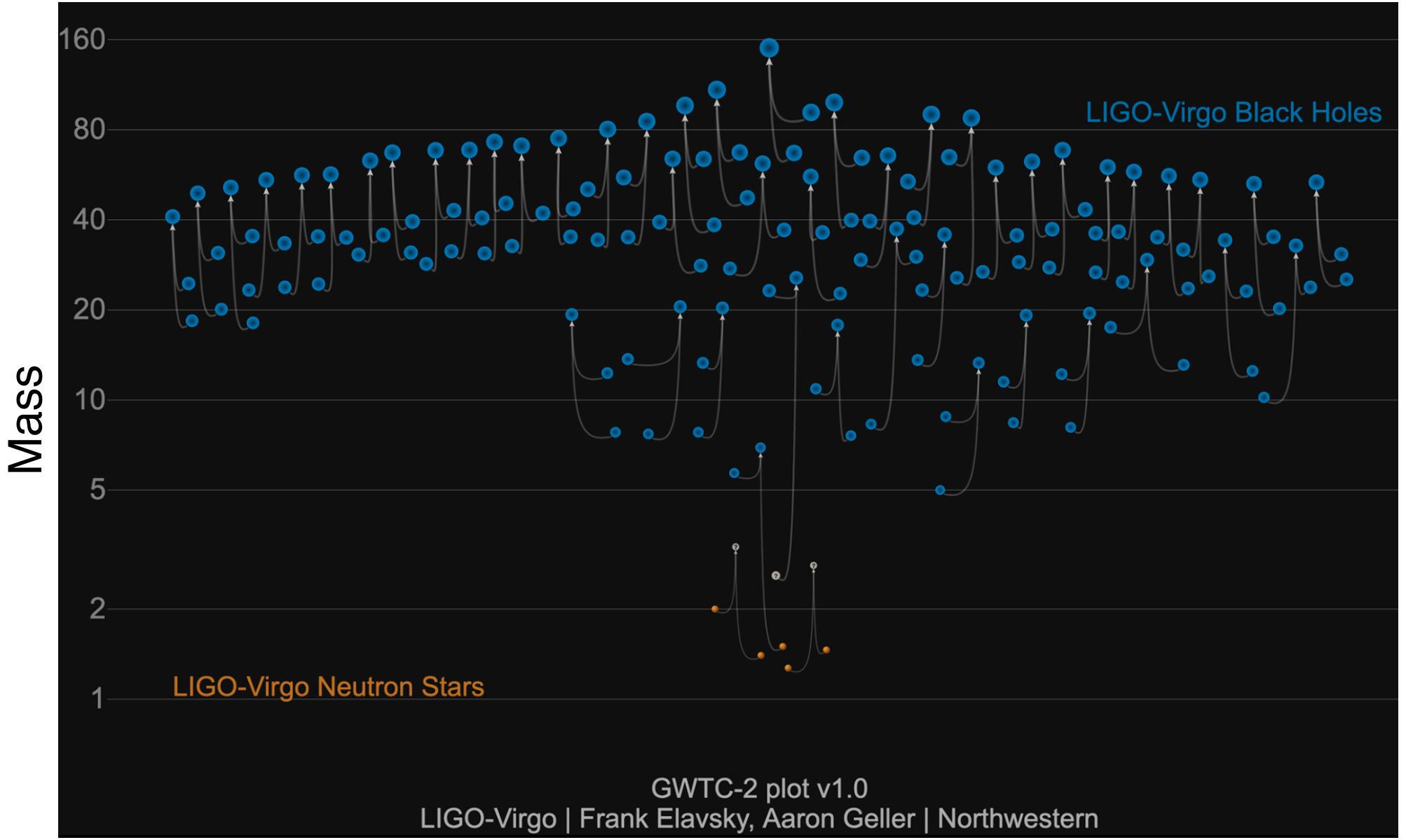
Mass
160
80
40
20
10
5
2
1
LIGO-Virgo Black Holes
LIGO-Virgo Neutron Stars
GWTC-2 plot v1.0
LIGO-Virgo | Frank Elavsky, Aaron Geller | Northwestern

Black Holes

- Astrophysical BHs forms from the gravitational collapse of a star. We know they exist. Their mass must be above the Chandrasekhar limit,

$$M > \mathcal{O}(1)\, M_\odot$$

- PBHs are formed in the early universe. Their mass can be small and they can still be around as long as they do not evaporate within the age of the universe

$$M > 10^{-18}\, M_\odot$$

- Can PBHs account for some of the LIGO/Virgo events?
- How to distinguish PBHs from astrophysical BHs?
- Can PBHs be the dark matter?

PBHs

Primordial black holes can compose all the dark matter (or a fraction of it)

$$f_{\rm PBH} = \Omega_{\rm PBH}/\Omega_{\rm DM}$$

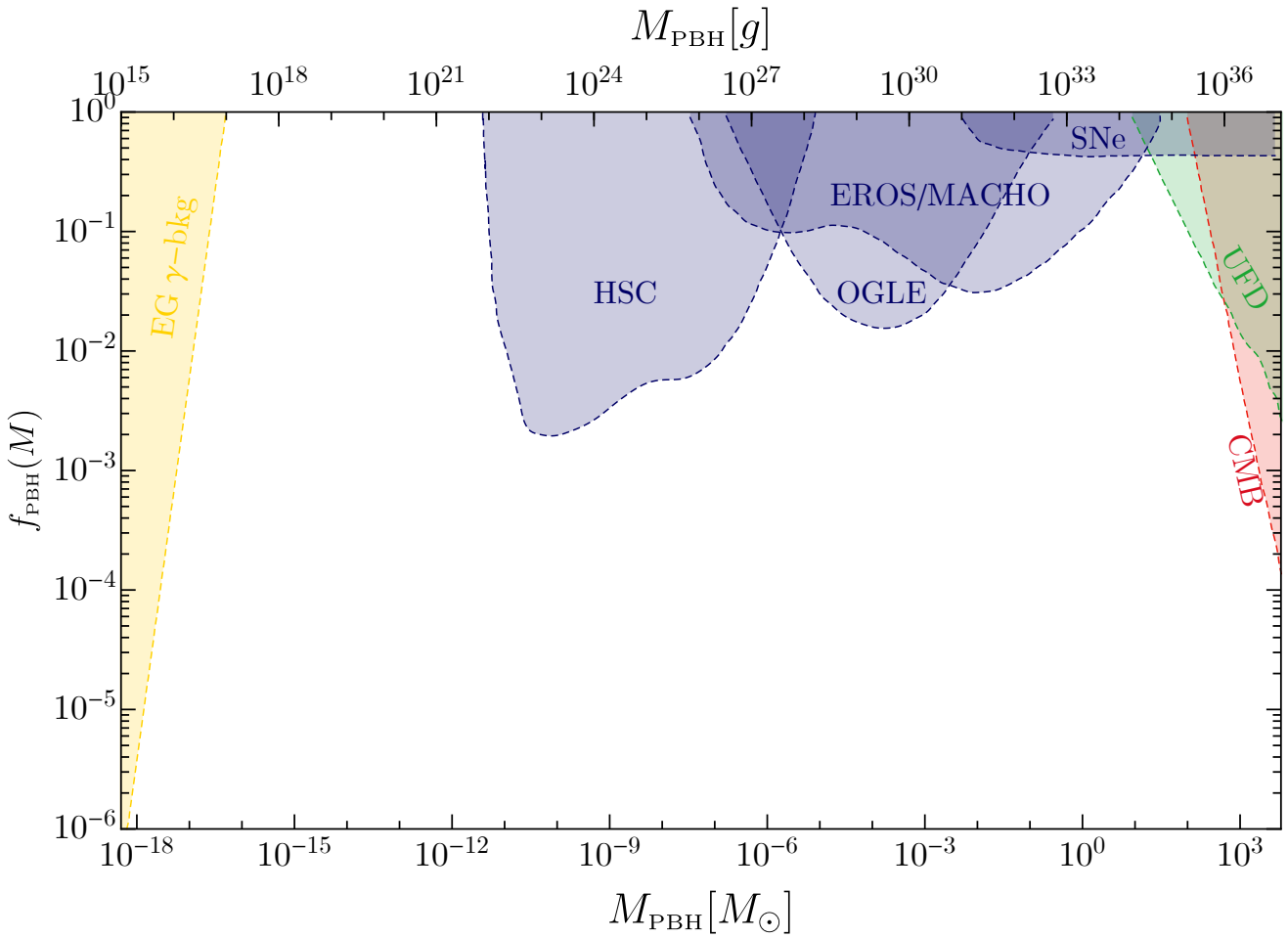

PBHs

Primordial black holes can compose all the dark matter (or a fraction of it)

$$f_{\rm PBH} = \Omega_{\rm PBH}/\Omega_{\rm DM}$$

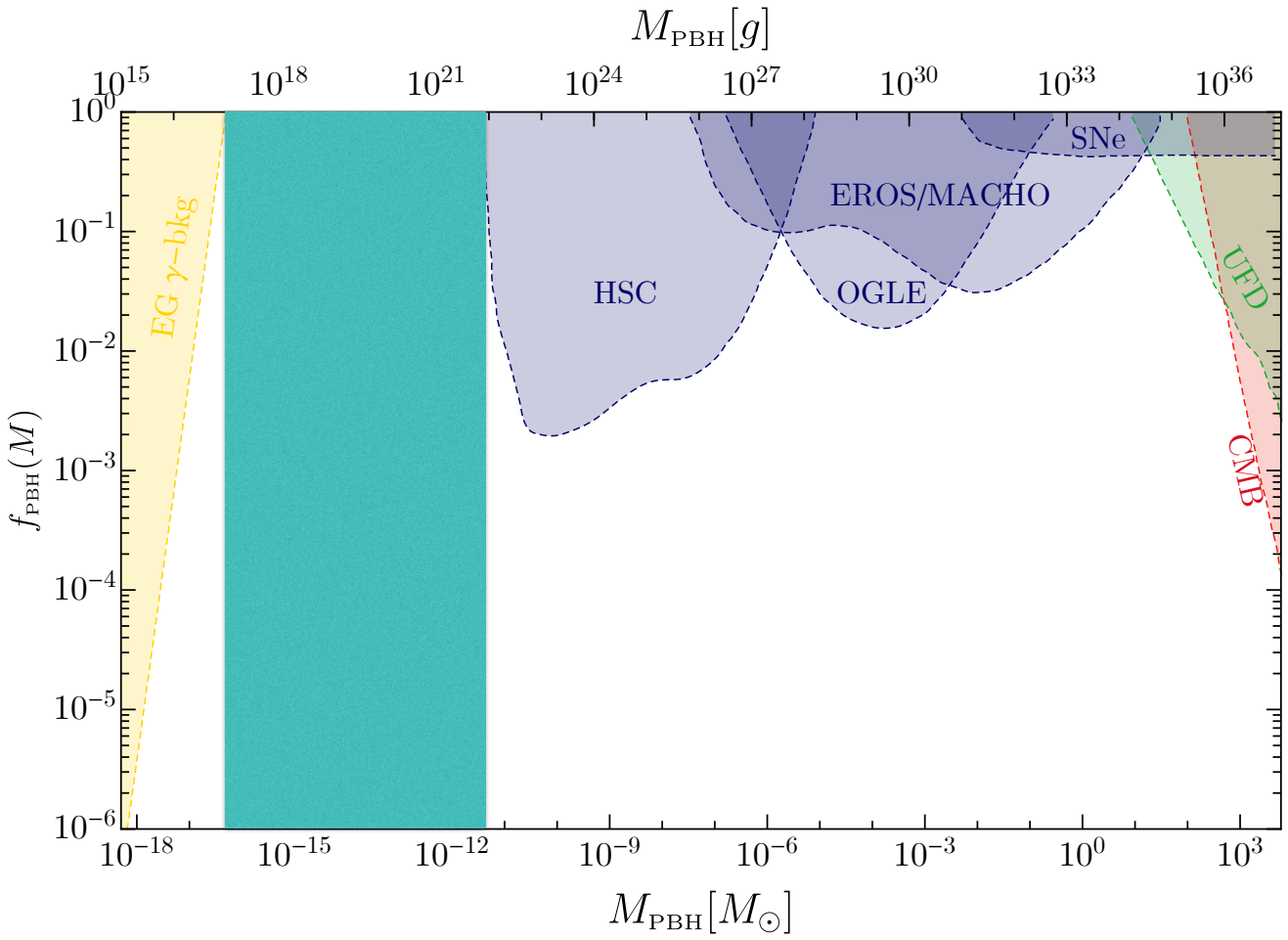

Assumption through out the seminar:

PBHs are originated from peaks of the density contrast

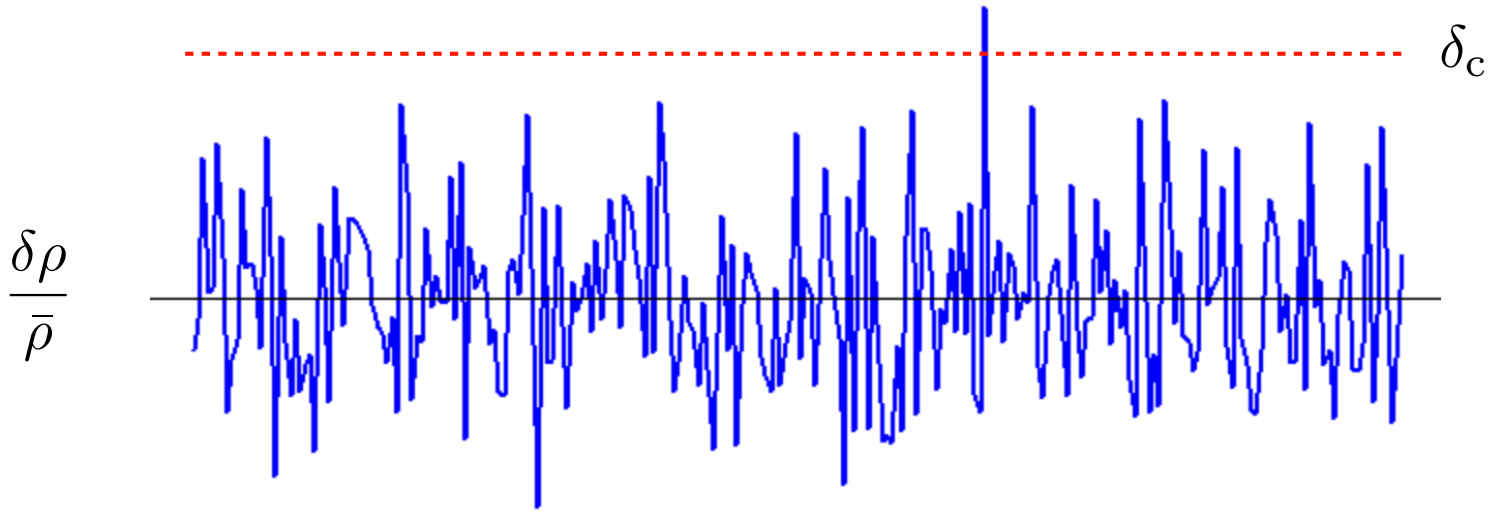

PBHs are rare events, tail of the distribution

One possible mechanism: large fluctuations from inflation

Assumption through out the seminar:

PBHs are originated from peaks of the density contrast

$$\frac{\delta\rho}{\rho} \gtrsim \delta_{\rm c} \qquad \frac{\delta\rho}{\bar{\rho}} \sim \frac{\nabla^2\zeta}{a^2H^2} \qquad M_{\rm PBH} \sim M_{\rm H}$$

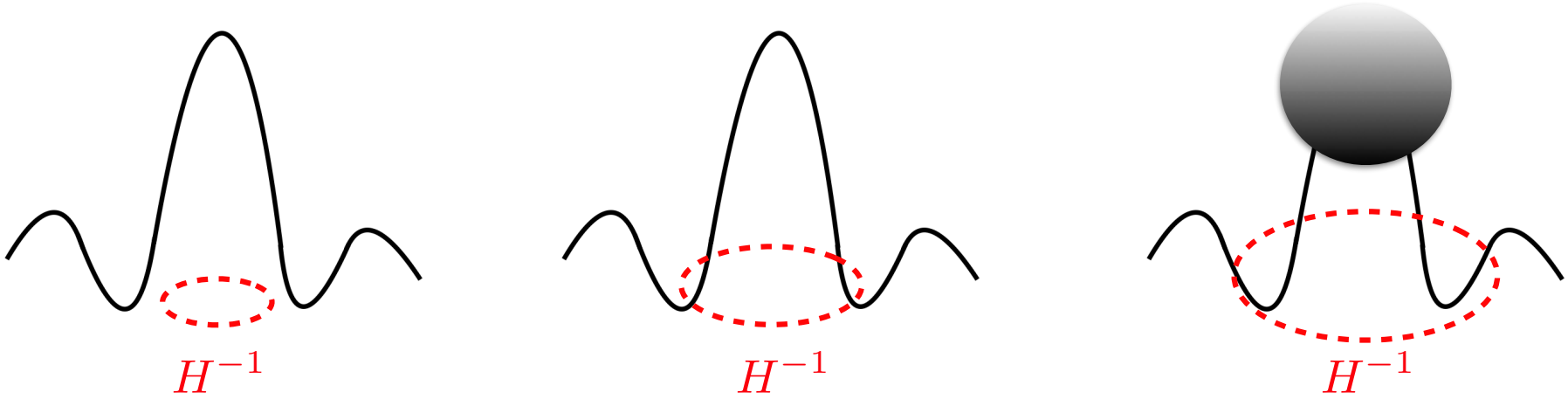

$$\beta(M) = \int_{\delta_{\rm c}}^{\infty} \frac{{\rm d}\delta}{\sqrt{2\pi}\sigma_\delta} e^{-\delta^2/2\sigma_\delta^2} \qquad \sigma_\delta^2 = \int_0^\infty {\rm d}\ln k W^2(k, R_H)\mathcal{P}_\delta(k)$$

Lot of work to go beyond the standard Gaussian lore

See Musco et al. (2020) for a simple prescription to calculate the threshold, including horizon crossing non-linear effects

Properties of PBHs at formation

The PBH mass function at formation

Mass distribution dependent on the curvature perturbation spectrum and statistical properties

Standard parametrisation

$$\psi(M_{\rm PBH}) = \frac{1}{\sqrt{2\pi} M_{\rm PBH}} \exp\left(-\frac{\ln^2(M_{\rm PBH}/M_c)}{2\sigma^2}\right)$$

May have different forms, e.g. if the curvature perturbation is broad, but still peaked at a given mass

De Luca et al. (2020)

The spin of PBHs at formation is small

- PBHs originate from peaks, that is from *maxima* of the local density contrast. Need peak theory to obtain the probability distribution of the spin

- The spin results from the action of the torques generated by the gravitational tidal forces upon horizon crossing

- It is a *first-order* effect in perturbation theory when accounting for the fact that the collapse is not spherical

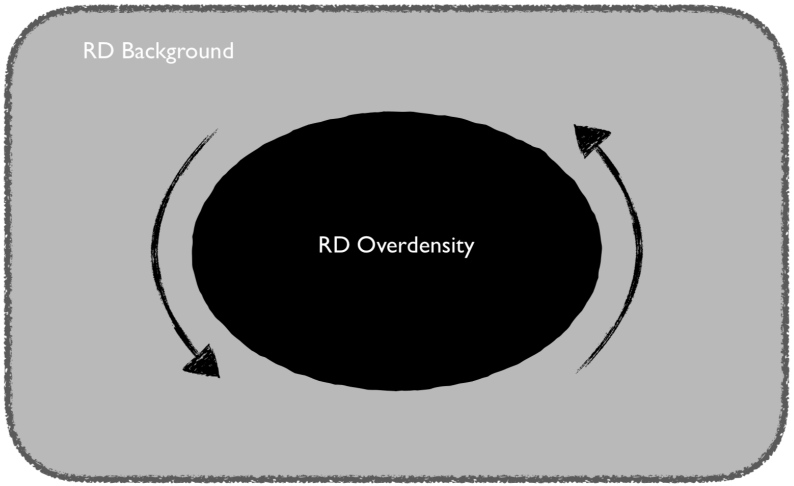

$$\vec{\chi} = \vec{S}/G_N M_{\rm PBH}^2$$

$$\chi_{\rm i} \sim 10^{-2}\sqrt{1-\gamma^2}$$

Shape of the density power spectrum

De Luca et al. (2018)

PBHs are not clustered at formation

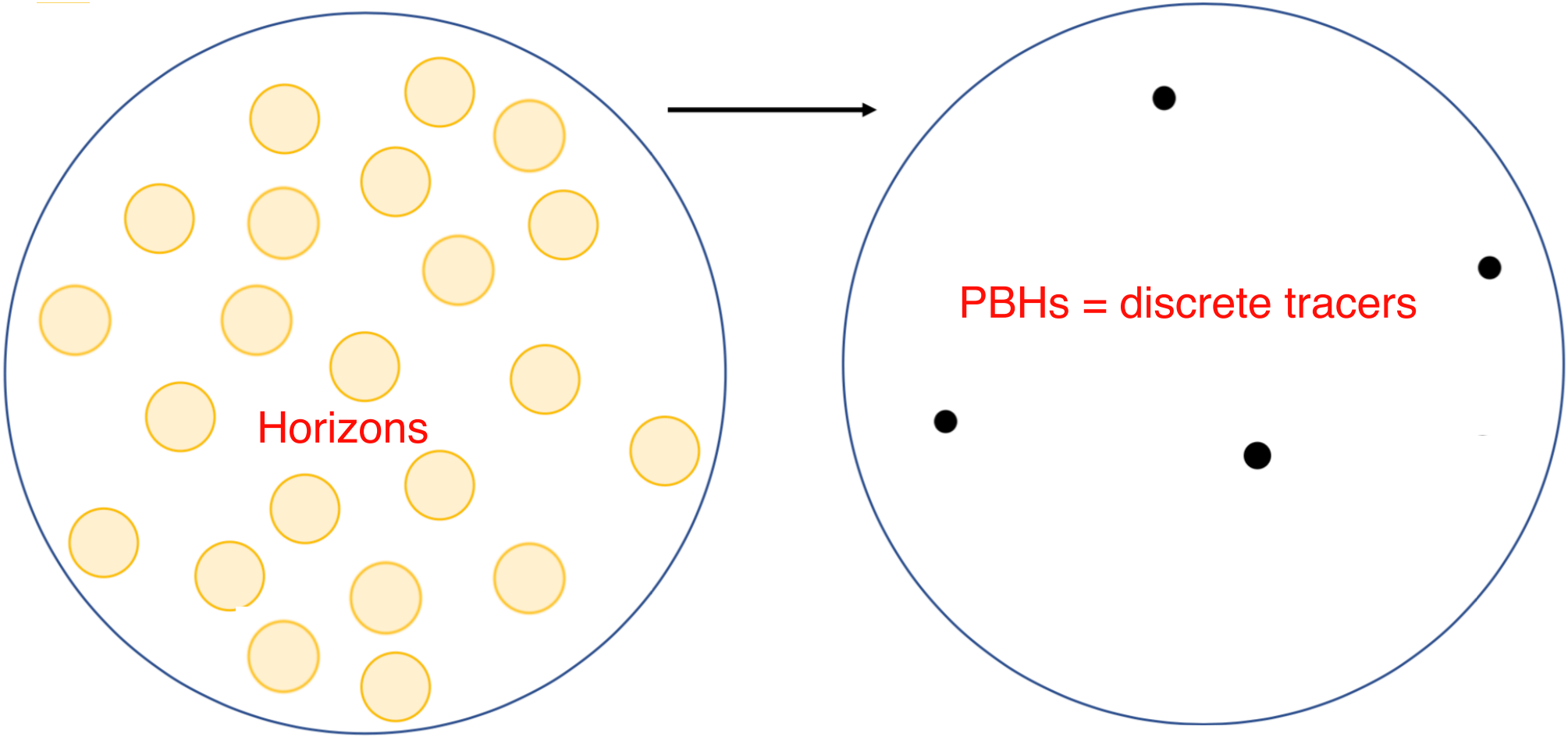

$$\left\langle \frac{\delta\rho_{\rm PBH}(\vec{x},z)}{\overline{\rho}_{\rm DM}} \frac{\delta\rho_{\rm PBH}(0,z)}{\overline{\rho}_{\rm DM}} \right\rangle = \frac{f_{\rm PBH}^2}{n_{\rm PBH}} \delta_{\rm D}(\vec{x}) + \xi(x,z)$$

with Desjaques (2018)

PBHs in the LIGO/Virgo mass range and GWs from mergers: the GWTC-2 catalogue

BH binary

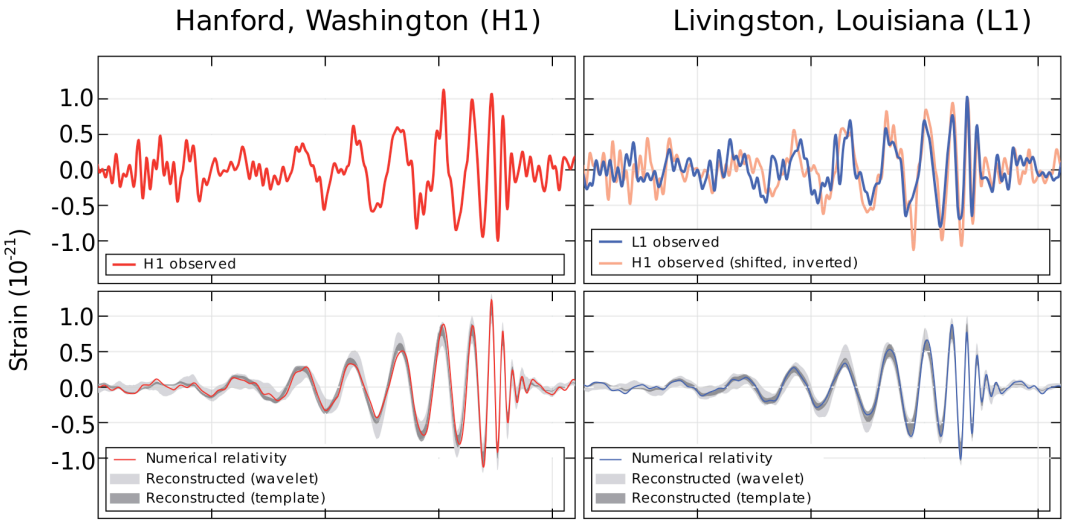

GW150914, LIGO (2016)

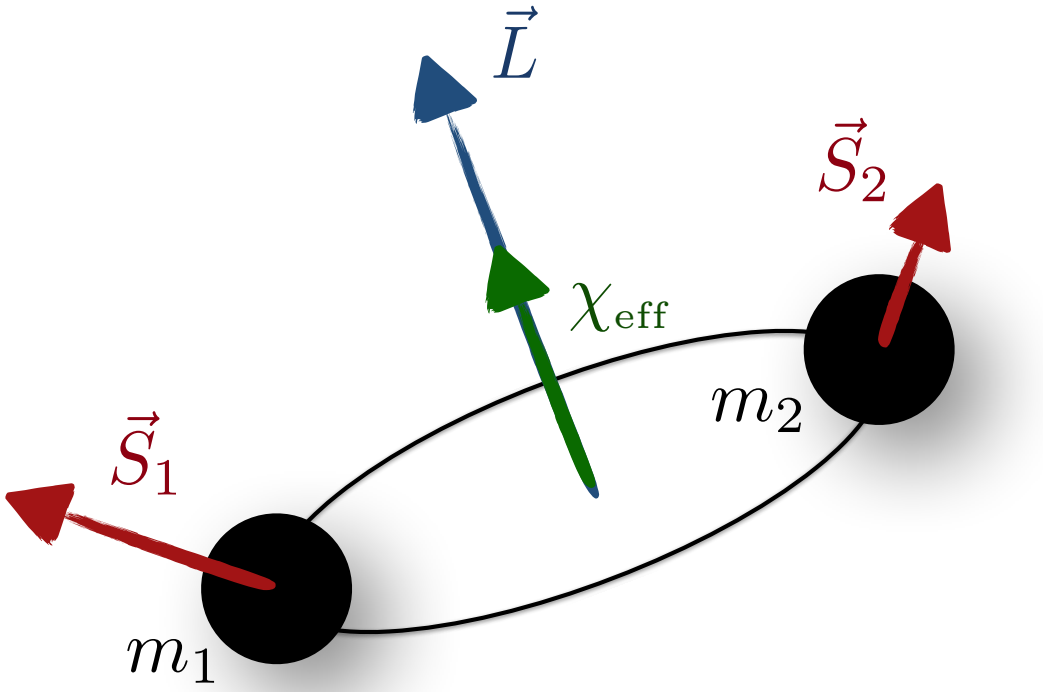

Waveforms dependent
on the binary event parameters

$$\mathcal{M} = \frac{(m_1 m_2)^{3/5}}{(m_1 + m_2)^{1/5}}$$

$$q = m_2/m_1$$

$$\chi_{\rm eff} = \frac{\vec{S}_1/m_1 + \vec{S}_2/m_2}{m_1 + m_2} \cdot \hat{L}$$

...

PBH evolution

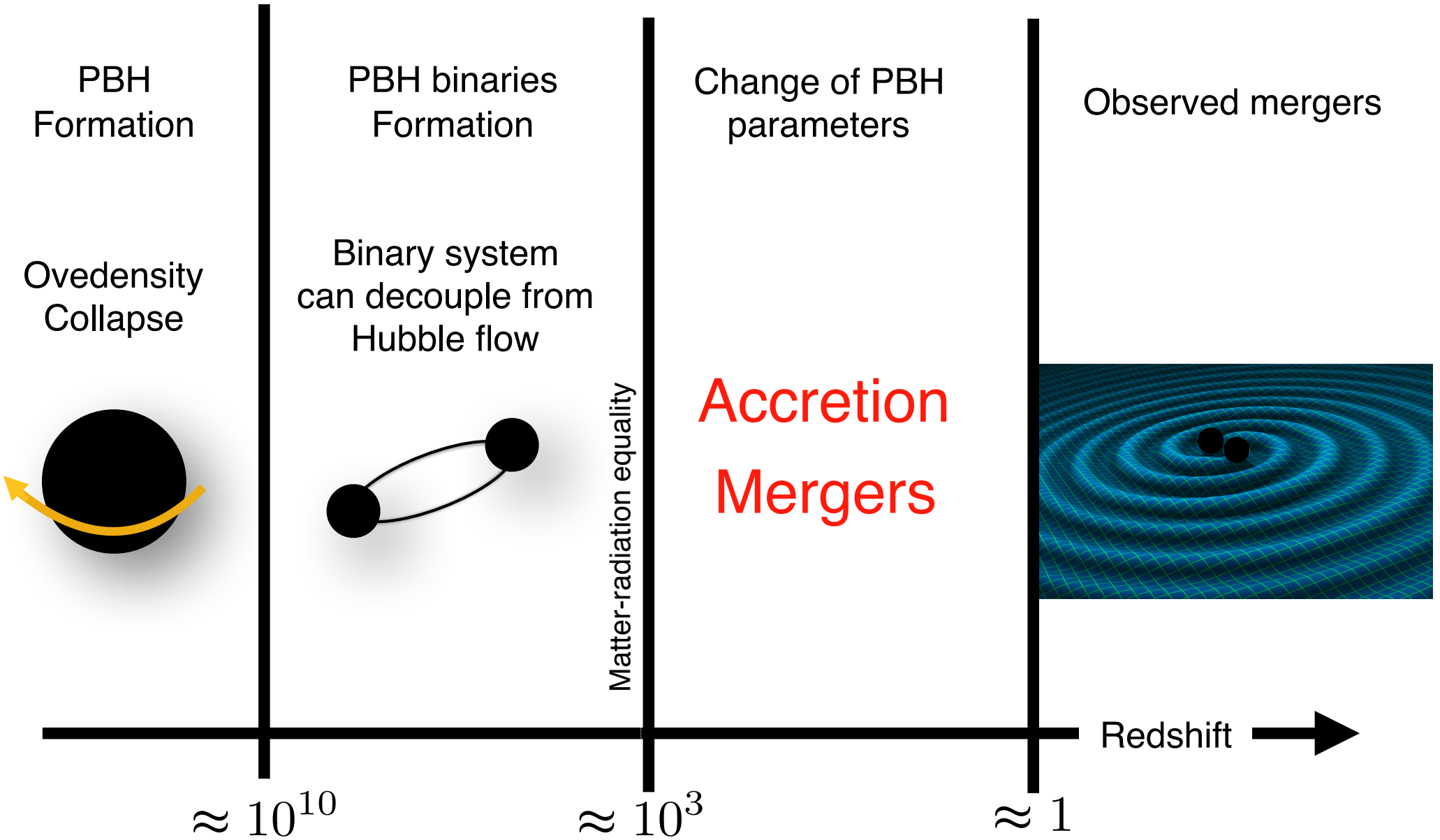

Accretion onto isolated PBHs

For $f_{\rm PBH} < 1$ PBHs coexist with another DM component in the universe

A DM halo builds up around the PBHs enhancing accretion

(larger gravitational potential well)

$$M_h(z) \approx 3 M_{\rm PBH} \left(\frac{1000}{1+z} \right)$$

Bondy-Hoyle accretion from the surrounding baryonic fluid

$$\dot{M} = 4\pi \lambda m_H n_{\rm gas} v_{\rm eff}^{-3} M^2$$

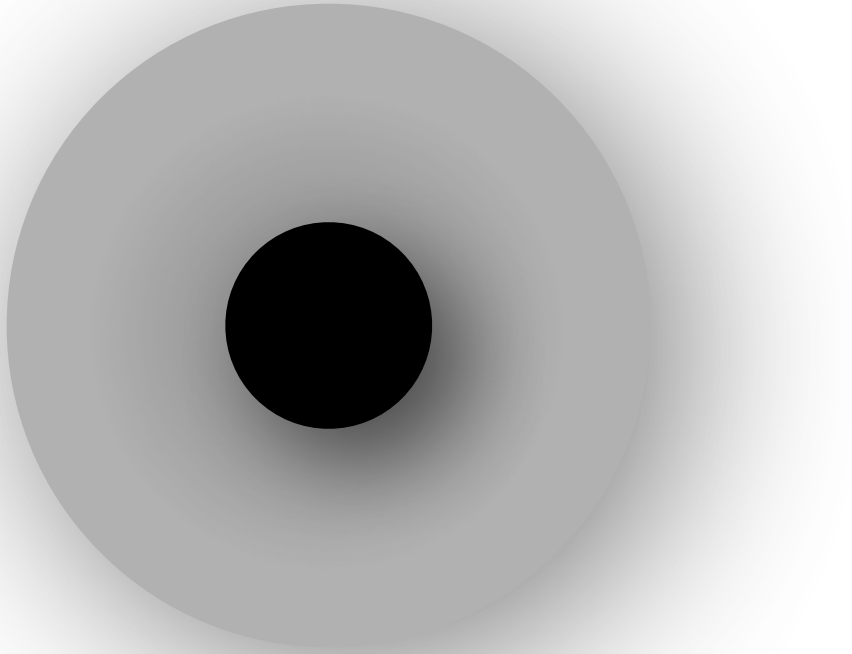

Ricotti et al. (2005)

Accretion onto PBH binaries

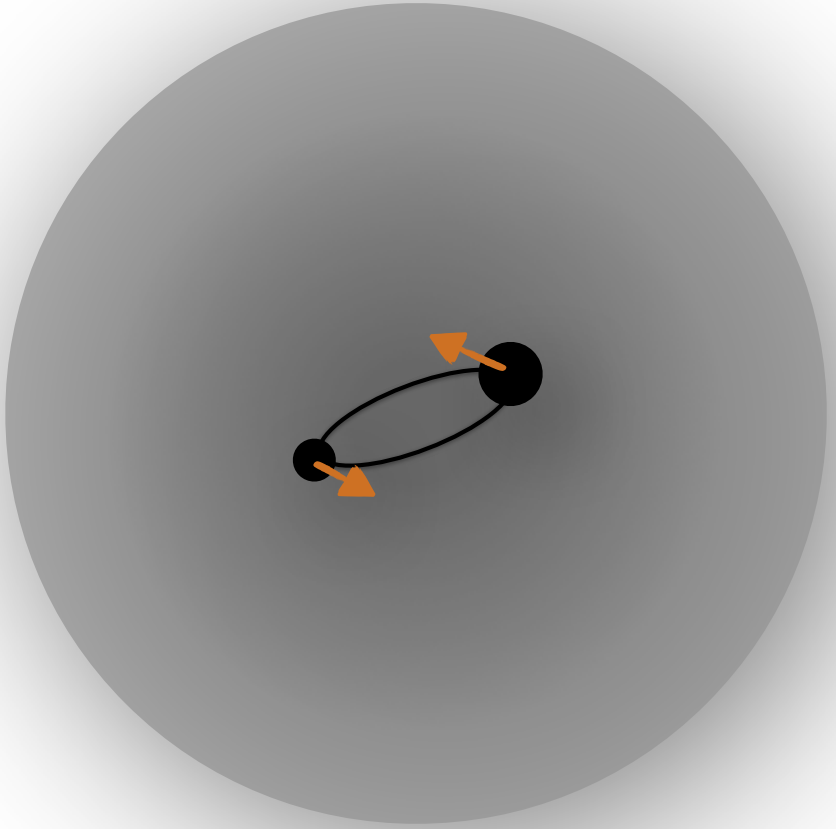

Accretion on the system enhances the gas density around the PBH binary

Accretion on the sigle PBH modulated by masses and orbital velocities

$$\dot{M}_1 = \dot{M} \frac{1}{\sqrt{2(1+q)}}$$

$$\dot{M}_2 = \dot{M} \sqrt{\frac{q}{2(1+q)}}$$

- The smaller PBH always experiences a larger relative accretion
- PBH can experience accretion for $M \gtrsim \mathcal{O}(10) M_\odot$

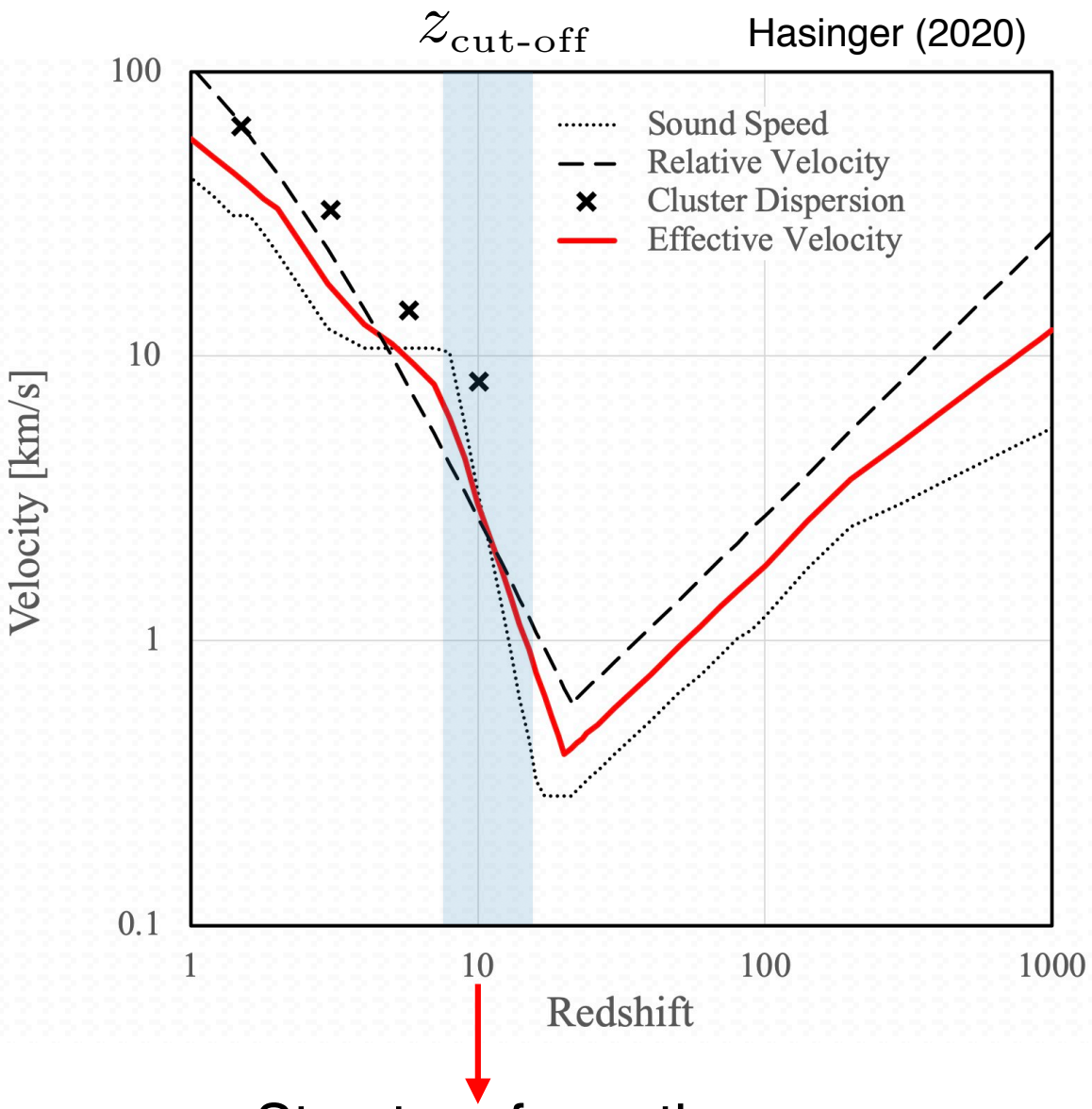

Structure formation
reionization epoch

- Virialised velocities
- Higher temperatures

$$\dot{M} \approx \left(v_{\mathrm{rel}}^2 + c_s^2\right)^{-3/2}$$

Strong suppression around

$z_{\mathrm{cut\text{-}off}}$

Uncertainties
in the accretion model
accounted for by
varying the cut-off

PBH mass function evolution

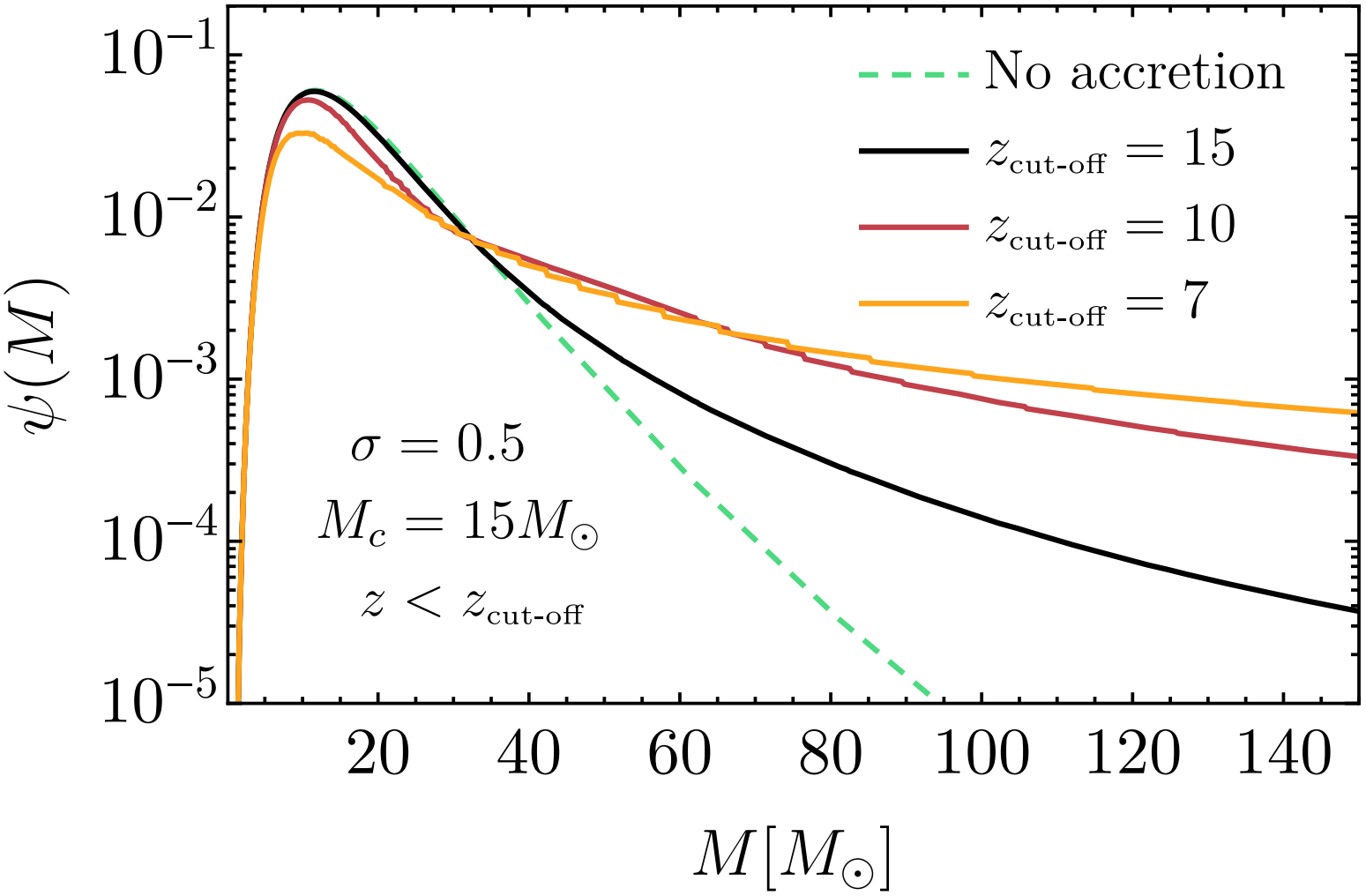

Non-linear mass evolution enhances large-mass tails

PBH mass evolution in binaries

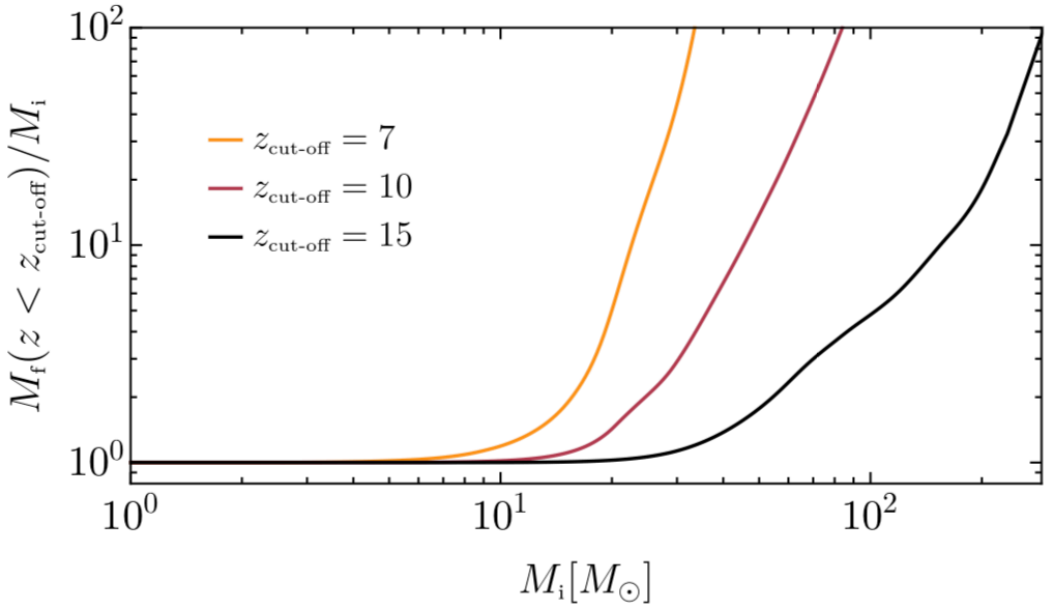

Large impact on masses, depending on the strength of accretion

$$\dot{q} = q\left(\frac{\dot{M}_2}{M_2} - \frac{\dot{M}_1}{M_1}\right)$$

Evolution of the mass ratio distribution towards equal-masses

Same MF initial width, at larger masses

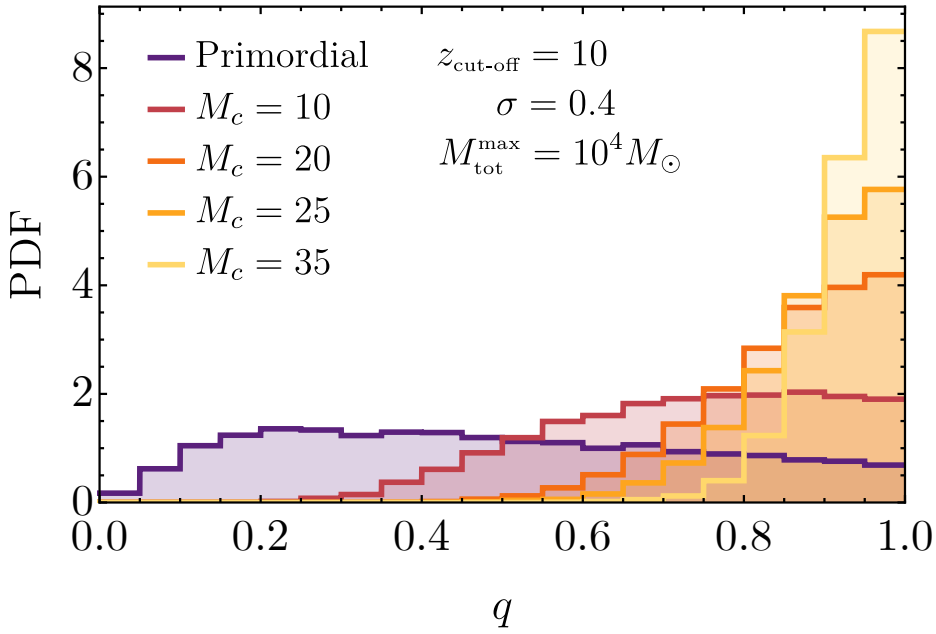

PBH spin evolution

If matter angular momentum is
large enough, an accreting disk forms,
leading to a spin growth

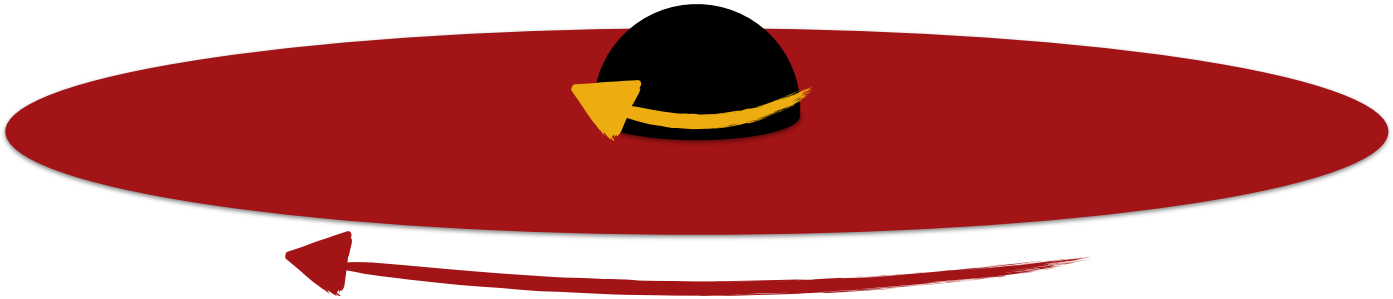

Angular momentum transfer
between gas and PBH

$$\dot{\chi} = g(\chi)\frac{\dot{M}}{M}$$

by solving the geodesic model of disk accretion

Bardeen et al. (1972)

Spins pushed towards extremality

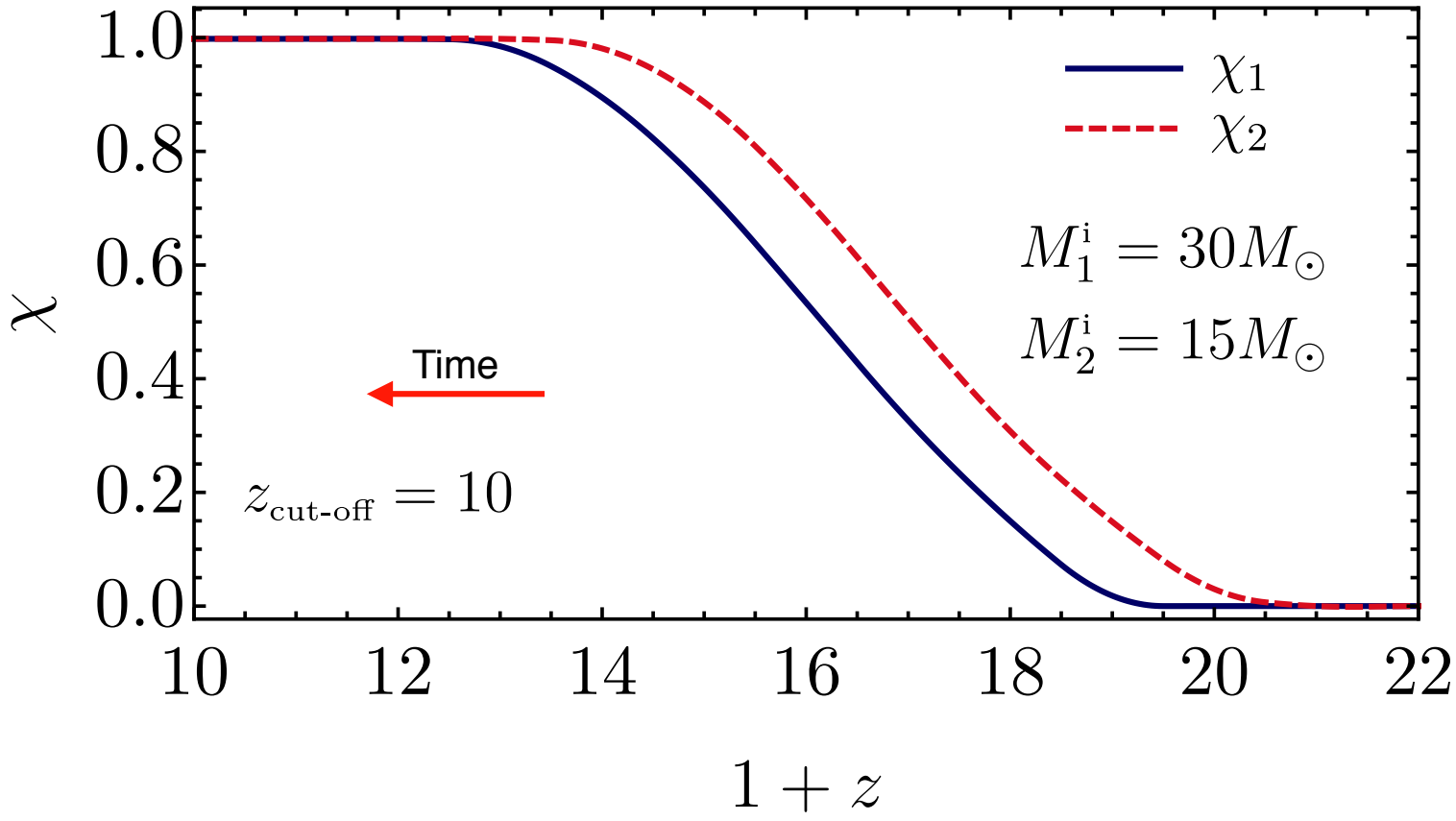

- Uncorrelated spin orientation
- Effective spin spreads around zero
- Accretion: low/large mass - low/large spin correlation

De Luca et al. (2020)

Merger rate

- Initial spatial Poisson distribution
- Random decoupling of binary systems

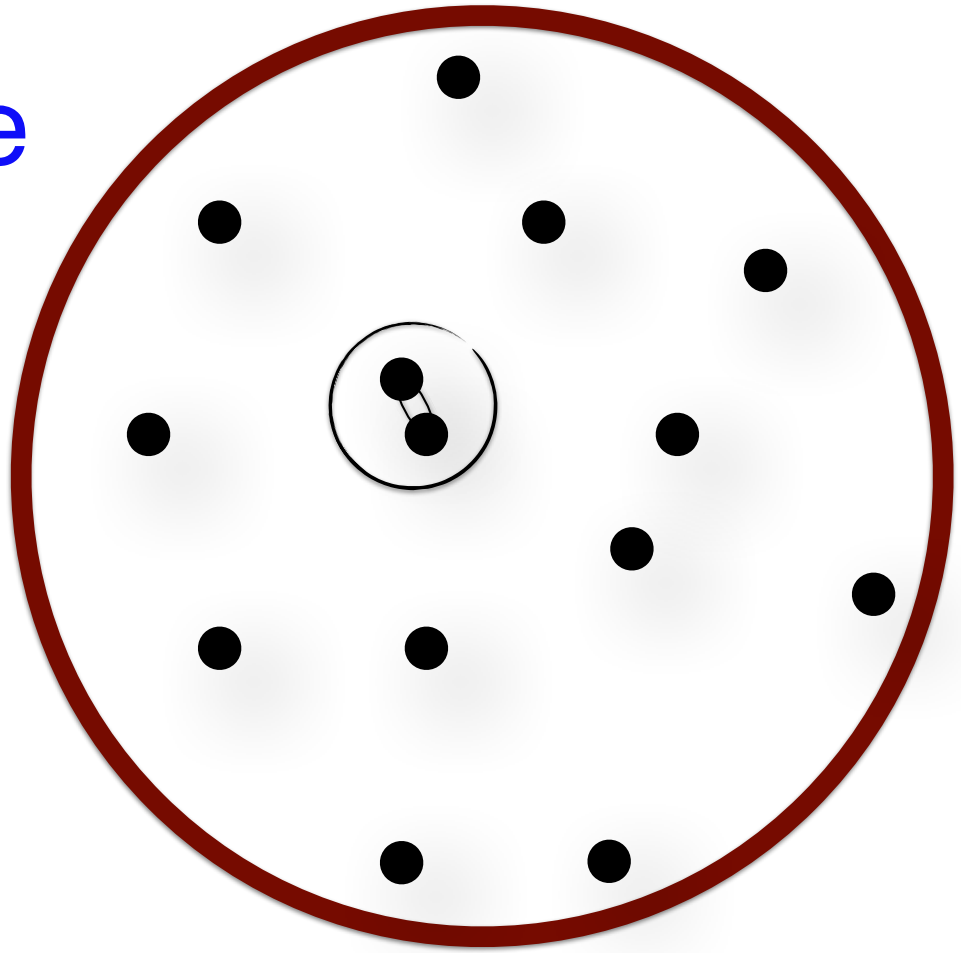

Compute probability of decoupling and the binary initial geometry

- Semi-major axis
- Eccentricity

Raidal et al (2018)

$$\frac{\mathrm{d}R}{\mathrm{d}m_1\mathrm{d}m_2} = \frac{1.6\times10^6}{\mathrm{Gpc^3\,yr}} f_{\rm PBH}^{\frac{53}{37}} \eta^{-\frac{34}{37}} \left(\frac{t}{t_0}\right)^{-\frac{34}{37}} \left(\frac{M_{\rm tot}}{M_\odot}\right)^{-\frac{32}{37}} S\left(M_{\rm tot}, f_{\rm PBH}\right) \mathcal{A}_{\rm acc}(m_j)\psi(m_1)\psi(m_2)$$

- Accretion hardens the binaries
- Larger masses leads to shorter mergers

De Luca et al. (2020)

GWTC-2=O1+O2+O3a

Event	M ($M_\odot$)	$\mathcal{M}$ ($M_\odot$)	m_1 ($M_\odot$)	m_2 ($M_\odot$)	$\chi_{\rm eff}$	$D_{\rm L}$ (Gpc)	z	$M_{\rm f}$ ($M_\odot$)	$\chi_{\rm f}$	$\Delta\Omega$ (deg^2)	SNR
GW190408_181802	$42.9^{+4.1}_{-2.9}$	$18.3^{+1.8}_{-1.2}$	$24.5^{+5.1}_{-3.4}$	$18.3^{+3.2}_{-3.5}$	$-0.03^{+0.13}_{-0.19}$	$1.58^{+0.40}_{-0.59}$	$0.30^{+0.06}_{-0.10}$	$41.0^{+3.8}_{-2.7}$	$0.67^{+0.06}_{-0.07}$	140	$15.3^{+0.2}_{-0.3}$
GW190412	$38.4^{+3.8}_{-3.7}$	$13.3^{+0.4}_{-0.3}$	$30.0^{+4.7}_{-5.1}$	$8.3^{+1.6}_{-0.9}$	$0.25^{+0.08}_{-0.11}$	$0.74^{+0.14}_{-0.17}$	$0.15^{+0.03}_{-0.03}$	$37.3^{+3.9}_{-3.9}$	$0.67^{+0.05}_{-0.06}$	21	$18.9^{+0.2}_{-0.3}$
GW190413_052954	$56.9^{+13.1}_{-8.9}$	$24.0^{+5.4}_{-3.7}$	$33.4^{+12.4}_{-7.4}$	$23.4^{+6.7}_{-6.3}$	$0.01^{+0.29}_{-0.33}$	$4.10^{+2.41}_{-1.89}$	$0.66^{+0.30}_{-0.27}$	$54.3^{+12.4}_{-8.4}$	$0.69^{+0.12}_{-0.13}$	1400	$8.9^{+0.4}_{-0.8}$
GW190413_134308	$76.1^{+15.9}_{-10.6}$	$31.9^{+7.3}_{-4.6}$	$45.4^{+13.6}_{-9.6}$	$30.9^{+10.2}_{-9.6}$	$-0.01^{+0.24}_{-0.28}$	$5.15^{+2.44}_{-2.34}$	$0.80^{+0.30}_{-0.31}$	$72.8^{+15.2}_{-10.3}$	$0.69^{+0.10}_{-0.12}$	520	$10.0^{+0.4}_{-0.5}$
GW190421_213856	$71.8^{+12.5}_{-8.6}$	$30.7^{+5.5}_{-3.9}$	$40.6^{+10.4}_{-6.6}$	$31.4^{+7.5}_{-8.2}$	$-0.05^{+0.23}_{-0.26}$	$3.15^{+1.37}_{-1.42}$	$0.53^{+0.18}_{-0.21}$	$68.6^{+11.7}_{-8.1}$	$0.68^{+0.10}_{-0.11}$	1000	$10.7^{+0.2}_{-0.4}$
GW190424_180648	$70.7^{+13.4}_{-9.8}$	$30.3^{+5.7}_{-4.2}$	$39.5^{+10.9}_{-6.9}$	$31.0^{+7.4}_{-7.3}$	$0.15^{+0.22}_{-0.22}$	$2.55^{+1.56}_{-1.33}$	$0.45^{+0.22}_{-0.21}$	$67.1^{+12.5}_{-9.2}$	$0.75^{+0.08}_{-0.09}$	26000	$10.4^{+0.2}_{-0.4}$
GW190425	$3.4^{+0.3}_{-0.1}$	$1.44^{+0.02}_{-0.02}$	$2.0^{+0.6}_{-0.3}$	$1.4^{+0.3}_{-0.3}$	$0.06^{+0.11}_{-0.05}$	$0.16^{+0.07}_{-0.07}$	$0.03^{+0.01}_{-0.02}$	–	–	9900	$12.4^{+0.3}_{-0.4}$
GW190426_152155	$7.2^{+3.5}_{-1.5}$	$2.41^{+0.08}_{-0.08}$	$5.7^{+4.0}_{-2.3}$	$1.5^{+0.8}_{-0.5}$	$-0.03^{+0.33}_{-0.30}$	$0.38^{+0.19}_{-0.16}$	$0.08^{+0.04}_{-0.03}$	–	–	1400	$8.7^{+0.5}_{-0.6}$
GW190503_185404	$71.3^{+9.3}_{-8.0}$	$30.1^{+4.2}_{-4.0}$	$42.9^{+9.2}_{-7.8}$	$28.5^{+7.5}_{-7.9}$	$-0.02^{+0.20}_{-0.26}$	$1.52^{+0.71}_{-0.66}$	$0.29^{+0.11}_{-0.11}$	$68.2^{+8.7}_{-7.5}$	$0.67^{+0.09}_{-0.12}$	94	$12.4^{+0.2}_{-0.3}$
GW190512_180714	$35.6^{+3.9}_{-3.4}$	$14.5^{+1.3}_{-1.0}$	$23.0^{+5.4}_{-5.7}$	$12.5^{+3.5}_{-2.5}$	$0.03^{+0.13}_{-0.13}$	$1.49^{+0.53}_{-0.59}$	$0.28^{+0.09}_{-0.10}$	$34.2^{+3.9}_{-3.4}$	$0.65^{+0.07}_{-0.07}$	230	$12.2^{+0.2}_{-0.4}$
GW190513_205428	$53.6^{+8.6}_{-5.9}$	$21.5^{+3.6}_{-1.9}$	$35.3^{+9.6}_{-9.0}$	$18.1^{+7.3}_{-4.2}$	$0.12^{+0.29}_{-0.18}$	$2.16^{+0.94}_{-0.80}$	$0.39^{+0.14}_{-0.13}$	$51.3^{+8.1}_{-5.8}$	$0.69^{+0.14}_{-0.12}$	490	$12.9^{+0.3}_{-0.4}$
GW190514_065416	$64.2^{+16.6}_{-9.6}$	$27.4^{+6.9}_{-4.3}$	$36.9^{+13.4}_{-7.3}$	$27.5^{+8.2}_{-7.7}$	$-0.16^{+0.28}_{-0.32}$	$4.93^{+2.76}_{-2.41}$	$0.77^{+0.34}_{-0.33}$	$61.6^{+16.0}_{-9.2}$	$0.64^{+0.11}_{-0.14}$	2400	$8.2^{+0.3}_{-0.6}$
GW190517_055101	$61.9^{+10.0}_{-9.6}$	$26.0^{+4.2}_{-4.0}$	$36.4^{+11.8}_{-7.8}$	$24.8^{+6.9}_{-7.1}$	$0.53^{+0.20}_{-0.19}$	$2.11^{+1.79}_{-1.00}$	$0.38^{+0.26}_{-0.16}$	$57.8^{+9.4}_{-9.1}$	$0.87^{+0.05}_{-0.07}$	460	$10.7^{+0.4}_{-0.6}$
GW190519_153544	$104.2^{+14.5}_{-14.9}$	$43.5^{+6.8}_{-6.8}$	$64.5^{+11.3}_{-13.2}$	$39.9^{+11.0}_{-10.6}$	$0.33^{+0.19}_{-0.22}$	$2.85^{+2.02}_{-1.14}$	$0.49^{+0.27}_{-0.17}$	$98.7^{+13.5}_{-14.2}$	$0.80^{+0.07}_{-0.12}$	770	$15.6^{+0.2}_{-0.3}$
GW190521	$157.9^{+37.4}_{-20.9}$	$66.9^{+15.5}_{-9.2}$	$91.4^{+29.3}_{-17.5}$	$66.8^{+20.7}_{-20.7}$	$0.06^{+0.31}_{-0.37}$	$4.53^{+2.30}_{-2.13}$	$0.72^{+0.29}_{-0.29}$	$150.3^{+35.8}_{-20.0}$	$0.73^{+0.11}_{-0.14}$	940	$14.2^{+0.3}_{-0.3}$
GW190521_074359	$74.4^{+6.8}_{-4.6}$	$31.9^{+3.1}_{-2.4}$	$42.1^{+5.9}_{-4.9}$	$32.7^{+5.4}_{-6.2}$	$0.09^{+0.10}_{-0.13}$	$1.28^{+0.38}_{-0.57}$	$0.25^{+0.06}_{-0.10}$	$70.7^{+6.4}_{-4.2}$	$0.72^{+0.05}_{-0.07}$	500	$25.8^{+0.1}_{-0.2}$
GW190527_092055	$58.5^{+27.9}_{-10.6}$	$24.2^{+11.9}_{-4.4}$	$36.2^{+19.1}_{-9.5}$	$22.8^{+12.7}_{-8.1}$	$0.13^{+0.29}_{-0.28}$	$3.10^{+4.85}_{-1.64}$	$0.53^{+0.61}_{-0.25}$	$55.9^{+26.4}_{-10.1}$	$0.73^{+0.12}_{-0.16}$	3800	$8.1^{+0.4}_{-1.0}$
GW190602_175927	$114.1^{+18.5}_{-15.7}$	$48.3^{+8.6}_{-8.0}$	$67.2^{+16.0}_{-12.6}$	$47.4^{+13.4}_{-16.6}$	$0.10^{+0.25}_{-0.25}$	$2.99^{+2.02}_{-1.26}$	$0.51^{+0.27}_{-0.19}$	$108.8^{+17.2}_{-14.8}$	$0.71^{+0.10}_{-0.13}$	720	$12.8^{+0.2}_{-0.3}$
GW190620_030421	$90.1^{+17.3}_{-12.1}$	$37.5^{+7.8}_{-5.7}$	$55.4^{+15.8}_{-12.0}$	$35.0^{+11.6}_{-11.4}$	$0.34^{+0.21}_{-0.25}$	$3.16^{+1.67}_{-1.43}$	$0.54^{+0.22}_{-0.21}$	$85.4^{+15.9}_{-11.4}$	$0.80^{+0.08}_{-0.14}$	6700	$12.1^{+0.3}_{-0.4}$
GW190630_185205	$58.8^{+4.7}_{-4.8}$	$24.8^{+2.1}_{-2.0}$	$35.0^{+6.9}_{-5.7}$	$23.6^{+5.2}_{-5.1}$	$0.10^{+0.12}_{-0.13}$	$0.93^{+0.56}_{-0.40}$	$0.19^{+0.10}_{-0.07}$	$56.1^{+4.5}_{-4.6}$	$0.70^{+0.06}_{-0.07}$	1300	$15.6^{+0.2}_{-0.3}$
GW190701_203306	$94.1^{+11.6}_{-9.3}$	$40.2^{+5.2}_{-4.7}$	$53.6^{+11.7}_{-7.8}$	$40.8^{+8.3}_{-11.5}$	$-0.06^{+0.23}_{-0.28}$	$2.14^{+0.79}_{-0.73}$	$0.38^{+0.12}_{-0.12}$	$90.0^{+10.8}_{-8.6}$	$0.67^{+0.09}_{-0.12}$	45	$11.3^{+0.2}_{-0.4}$
GW190706_222641	$101.6^{+17.9}_{-13.5}$	$42.0^{+8.4}_{-6.2}$	$64.0^{+15.2}_{-15.2}$	$38.5^{+12.5}_{-12.4}$	$0.32^{+0.25}_{-0.30}$	$5.07^{+2.57}_{-2.11}$	$0.79^{+0.31}_{-0.28}$	$96.3^{+16.7}_{-13.2}$	$0.80^{+0.08}_{-0.17}$	610	$12.6^{+0.2}_{-0.4}$
GW190707_093326	$20.0^{+1.9}_{-1.3}$	$8.5^{+0.6}_{-0.4}$	$11.5^{+3.3}_{-1.7}$	$8.4^{+1.4}_{-1.6}$	$-0.05^{+0.10}_{-0.08}$	$0.80^{+0.37}_{-0.38}$	$0.16^{+0.07}_{-0.07}$	$19.2^{+1.9}_{-1.3}$	$0.66^{+0.03}_{-0.04}$	1300	$13.3^{+0.2}_{-0.4}$
GW190708_232457	$30.8^{+2.5}_{-1.8}$	$13.1^{+0.9}_{-0.6}$	$17.5^{+4.7}_{-2.3}$	$13.1^{+2.0}_{-2.7}$	$0.02^{+0.10}_{-0.08}$	$0.90^{+0.33}_{-0.40}$	$0.18^{+0.06}_{-0.07}$	$29.4^{+2.5}_{-1.7}$	$0.69^{+0.04}_{-0.04}$	14000	$13.1^{+0.2}_{-0.3}$
GW190719_215514	$55.8^{+16.3}_{-10.0}$	$22.7^{+5.9}_{-3.7}$	$35.2^{+16.9}_{-9.9}$	$20.2^{+8.1}_{-6.5}$	$0.35^{+0.28}_{-0.32}$	$4.61^{+2.84}_{-2.17}$	$0.73^{+0.35}_{-0.30}$	$52.9^{+15.6}_{-9.5}$	$0.80^{+0.10}_{-0.16}$	2300	$8.3^{+0.3}_{-1.0}$
GW190720_000836	$21.3^{+4.3}_{-2.3}$	$8.9^{+0.5}_{-0.8}$	$13.3^{+6.6}_{-3.0}$	$7.8^{+2.2}_{-2.2}$	$0.18^{+0.14}_{-0.12}$	$0.81^{+0.71}_{-0.33}$	$0.16^{+0.12}_{-0.06}$	$20.3^{+4.5}_{-2.3}$	$0.72^{+0.06}_{-0.05}$	510	$11.0^{+0.3}_{-0.8}$
GW190727_060333	$65.8^{+10.9}_{-7.4}$	$28.1^{+4.9}_{-3.4}$	$37.2^{+9.4}_{-5.9}$	$28.8^{+6.6}_{-7.9}$	$0.12^{+0.26}_{-0.25}$	$3.60^{+1.56}_{-1.51}$	$0.60^{+0.20}_{-0.22}$	$62.6^{+10.2}_{-7.0}$	$0.73^{+0.10}_{-0.10}$	860	$11.9^{+0.3}_{-0.5}$
GW190728_064510	$20.5^{+4.5}_{-1.3}$	$8.6^{+0.5}_{-0.3}$	$12.2^{+7.1}_{-2.2}$	$8.1^{+1.7}_{-2.6}$	$0.12^{+0.19}_{-0.07}$	$0.89^{+0.25}_{-0.37}$	$0.18^{+0.05}_{-0.07}$	$19.5^{+4.6}_{-1.3}$	$0.71^{+0.04}_{-0.04}$	410	$13.0^{+0.2}_{-0.4}$
GW190731_140936	$67.1^{+15.3}_{-10.2}$	$28.4^{+6.8}_{-4.5}$	$39.3^{+11.8}_{-8.2}$	$28.0^{+8.9}_{-8.4}$	$0.08^{+0.24}_{-0.24}$	$3.97^{+2.56}_{-2.07}$	$0.65^{+0.32}_{-0.30}$	$63.9^{+14.4}_{-9.8}$	$0.71^{+0.10}_{-0.12}$	3000	$8.6^{+0.2}_{-0.5}$
GW190803_022701	$62.7^{+11.8}_{-8.4}$	$26.7^{+5.2}_{-3.8}$	$36.1^{+10.2}_{-6.7}$	$26.7^{+7.1}_{-7.6}$	$-0.01^{+0.25}_{-0.26}$	$3.69^{+2.04}_{-1.69}$	$0.61^{+0.26}_{-0.24}$	$59.9^{+11.2}_{-7.9}$	$0.69^{+0.10}_{-0.11}$	1500	$8.6^{+0.3}_{-0.5}$
GW190814	$25.8^{+1.0}_{-0.9}$	$6.09^{+0.06}_{-0.06}$	$23.2^{+1.1}_{-1.0}$	$2.59^{+0.08}_{-0.09}$	$0.00^{+0.06}_{-0.06}$	$0.24^{+0.04}_{-0.05}$	$0.05^{+0.009}_{-0.010}$	$25.6^{+1.0}_{-0.9}$	$0.28^{+0.02}_{-0.02}$	19	$24.9^{+0.1}_{-0.2}$
GW190828_063405	$57.5^{+7.5}_{-4.4}$	$24.8^{+3.3}_{-2.0}$	$31.8^{+5.8}_{-3.9}$	$25.9^{+4.4}_{-4.6}$	$0.19^{+0.15}_{-0.16}$	$2.22^{+0.63}_{-0.95}$	$0.40^{+0.09}_{-0.15}$	$54.5^{+6.9}_{-4.0}$	$0.76^{+0.06}_{-0.07}$	520	$16.2^{+0.2}_{-0.3}$
GW190828_065509	$34.1^{+5.5}_{-4.5}$	$13.3^{+1.2}_{-0.9}$	$23.8^{+7.2}_{-7.0}$	$10.2^{+3.5}_{-2.1}$	$0.08^{+0.16}_{-0.16}$	$1.66^{+0.63}_{-0.61}$	$0.31^{+0.10}_{-0.10}$	$32.9^{+5.7}_{-4.5}$	$0.65^{+0.09}_{-0.08}$	640	$10.0^{+0.3}_{-0.5}$
GW190909_114149	$71.2^{+54.3}_{-15.0}$	$29.5^{+17.5}_{-6.3}$	$43.2^{+50.7}_{-12.2}$	$27.6^{+13.0}_{-10.9}$	$-0.03^{+0.44}_{-0.36}$	$4.77^{+3.70}_{-2.66}$	$0.75^{+0.45}_{-0.37}$	$68.3^{+52.5}_{-14.5}$	$0.68^{+0.16}_{-0.18}$	4200	$8.1^{+0.4}_{-0.7}$
GW190910_112807	$78.7^{+9.5}_{-9.0}$	$33.9^{+4.3}_{-3.9}$	$43.5^{+7.6}_{-6.2}$	$35.1^{+6.3}_{-7.0}$	$0.02^{+0.19}_{-0.18}$	$1.57^{+1.07}_{-0.64}$	$0.29^{+0.17}_{-0.11}$	$75.0^{+8.7}_{-8.5}$	$0.70^{+0.08}_{-0.07}$	10000	$14.1^{+0.2}_{-0.3}$
GW190915_235702	$59.5^{+7.5}_{-6.2}$	$25.1^{+3.1}_{-2.6}$	$34.9^{+9.5}_{-6.2}$	$24.4^{+5.5}_{-6.0}$	$0.03^{+0.19}_{-0.24}$	$1.70^{+0.71}_{-0.64}$	$0.32^{+0.11}_{-0.11}$	$56.8^{+7.1}_{-5.8}$	$0.71^{+0.09}_{-0.11}$	380	$13.6^{+0.2}_{-0.3}$
GW190924_021846	$13.9^{+5.1}_{-0.9}$	$5.8^{+0.2}_{-0.2}$	$8.8^{+7.0}_{-2.0}$	$5.0^{+1.3}_{-1.9}$	$0.03^{+0.30}_{-0.09}$	$0.57^{+0.22}_{-0.22}$	$0.12^{+0.04}_{-0.04}$	$13.3^{+5.2}_{-1.0}$	$0.67^{+0.05}_{-0.05}$	380	$11.5^{+0.3}_{-0.4}$
GW190929_012149	$90.6^{+21.2}_{-14.1}$	$34.3^{+8.6}_{-6.5}$	$64.7^{+22.4}_{-18.9}$	$25.7^{+14.4}_{-9.7}$	$0.03^{+0.27}_{-0.27}$	$3.68^{+2.98}_{-1.68}$	$0.61^{+0.38}_{-0.24}$	$87.5^{+20.7}_{-14.1}$	$0.64^{+0.17}_{-0.23}$	1800	$9.8^{+0.8}_{-0.6}$
GW190930_133541	$20.3^{+9.0}_{-1.5}$	$8.5^{+0.5}_{-0.5}$	$12.3^{+12.5}_{-2.3}$	$7.8^{+1.7}_{-3.3}$	$0.14^{+0.31}_{-0.15}$	$0.78^{+0.37}_{-0.33}$	$0.16^{+0.07}_{-0.06}$	$19.3^{+9.3}_{-1.5}$	$0.72^{+0.07}_{-0.06}$	1800	$9.5^{+0.3}_{-0.5}$

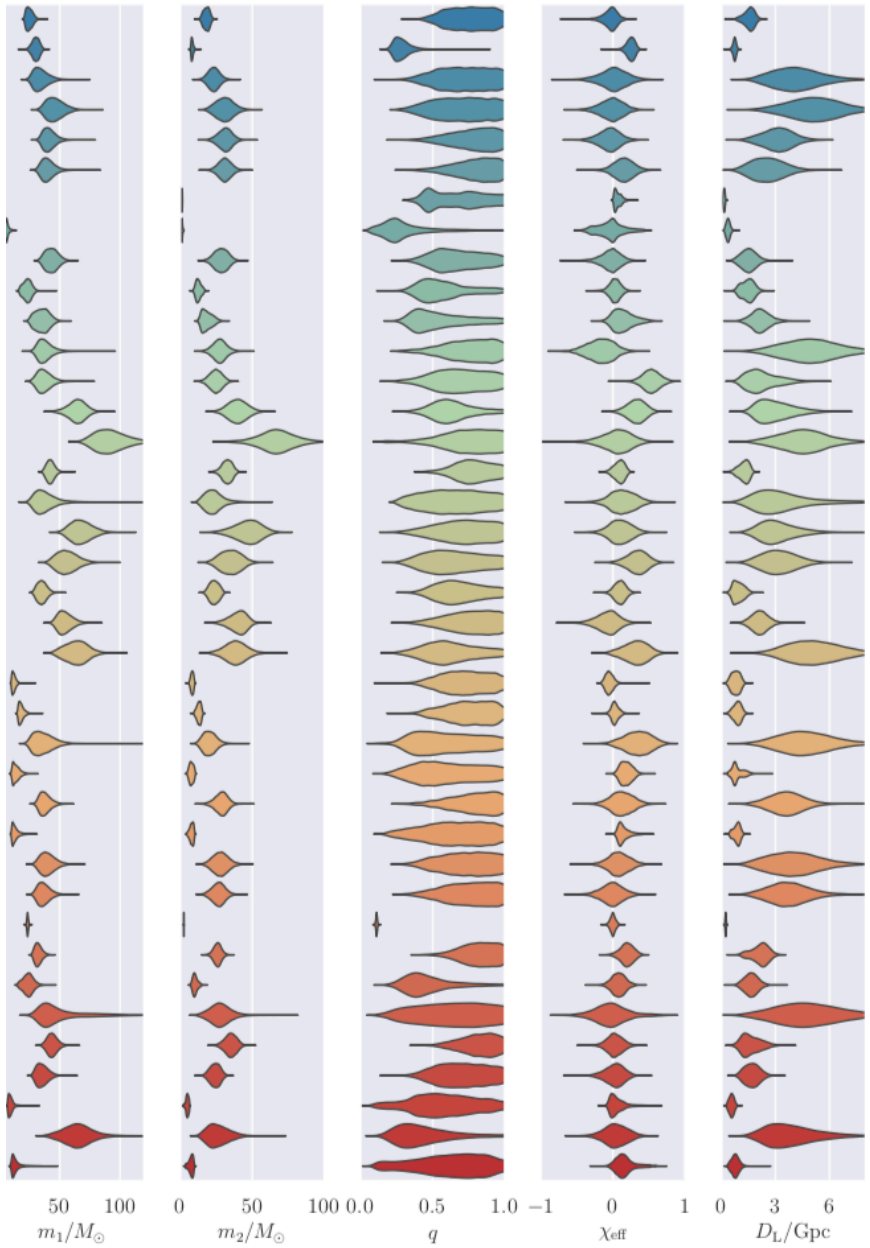

Bayesian evidence in GWTC-2 catalogue

- Hierarchical Bayesian analysis in the GWTC-2 catalogue to investigate the presence of Astro BHs and PBH events in the data

De Luca et al. (2021)

- Same exercise done with more astrophysical models: multiple channels needed

Zevin et al. (2021)

Bayesian evidence in GWTC-2 catalogue

- Hierarchical Bayesian analysis in the GWTC-2 catalogue to investigate the presence of Astro BHs and PBH events in the data

De Luca et al. (2021)

- Same exercise done with more astrophysical models: multiple channels needed

Zevin et al. (2021)

- Astrophysical phenomenological Truncated plus Gaussian-spin model adopted as well by the LIGO-Virgo collaboration

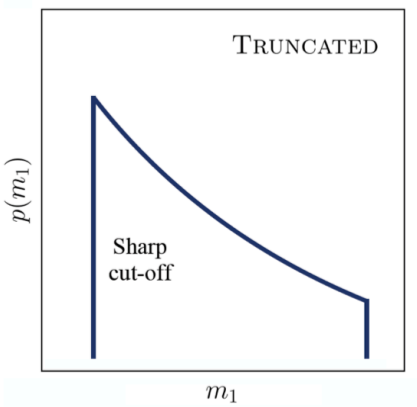

$$\frac{\mathrm{d}R_{\mathrm{ABH}}}{\mathrm{d}m_1\mathrm{d}m_2\mathrm{d}z} = \mathcal{N}R_0(1+z)^{\kappa}(m_1+m_2)^{\alpha}\left[\frac{m_1 m_2}{(m_1+m_2)^2}\right]^{\beta}\psi(m_1)\psi(m_2)$$

$$\psi(m|\zeta, m_{\mathrm{min}}, m_{\mathrm{max}}) \propto m^{-\zeta} \qquad \text{for} \qquad m_{\mathrm{min}} < m < m_{\mathrm{max}}$$

Bayesian evidence in GWTC-2 catalogue

- Hierarchical Bayesian analysis in the GWTC-2 catalogue to investigate the presence of Astro BHs and PBH events in the data

De Luca et al. (2021)

- Same exercise done with more astrophysical models: multiple channels needed

Zevin et al. (2021)

- Astrophysical phenomenological Truncated plus Gaussian-spin Model adopted as well by the LIGO-Virgo collaboration

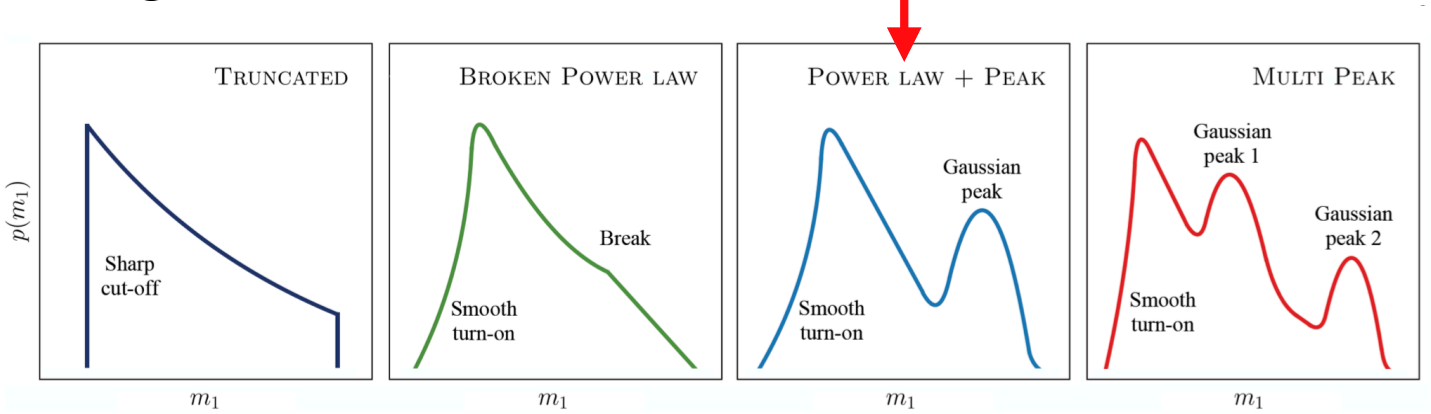

Bayesian evidence in GWTC-2

Event parameters $\vec{\theta}$

m_1 m_2 $\chi_{\rm eff}$ z

Population Hyperparameters $\vec{\lambda}$

M_c σ $f_{\rm PBH}$ $z_{\text{cut-off}}$ R_0 κ α β ζ $m_{\rm min}$ $m_{\rm max}$ $\mu_{\chi_{\rm eft}}$ $\sigma_{\chi_{\rm eff}}$

$$p(\vec{\lambda}|\vec{d}) \propto p(\vec{\lambda}) \int \mathrm{d}\vec{\theta}\, p(\vec{d}|\vec{\theta}) p_{\rm pop}(\vec{\theta}|\vec{\lambda})$$

Posterior distribution

Hyperparameter prior

Single event likelihood

Population likelihood (ML)

De Luca et al. (2021)

Population posterior distributions

De Luca et al. (2021)

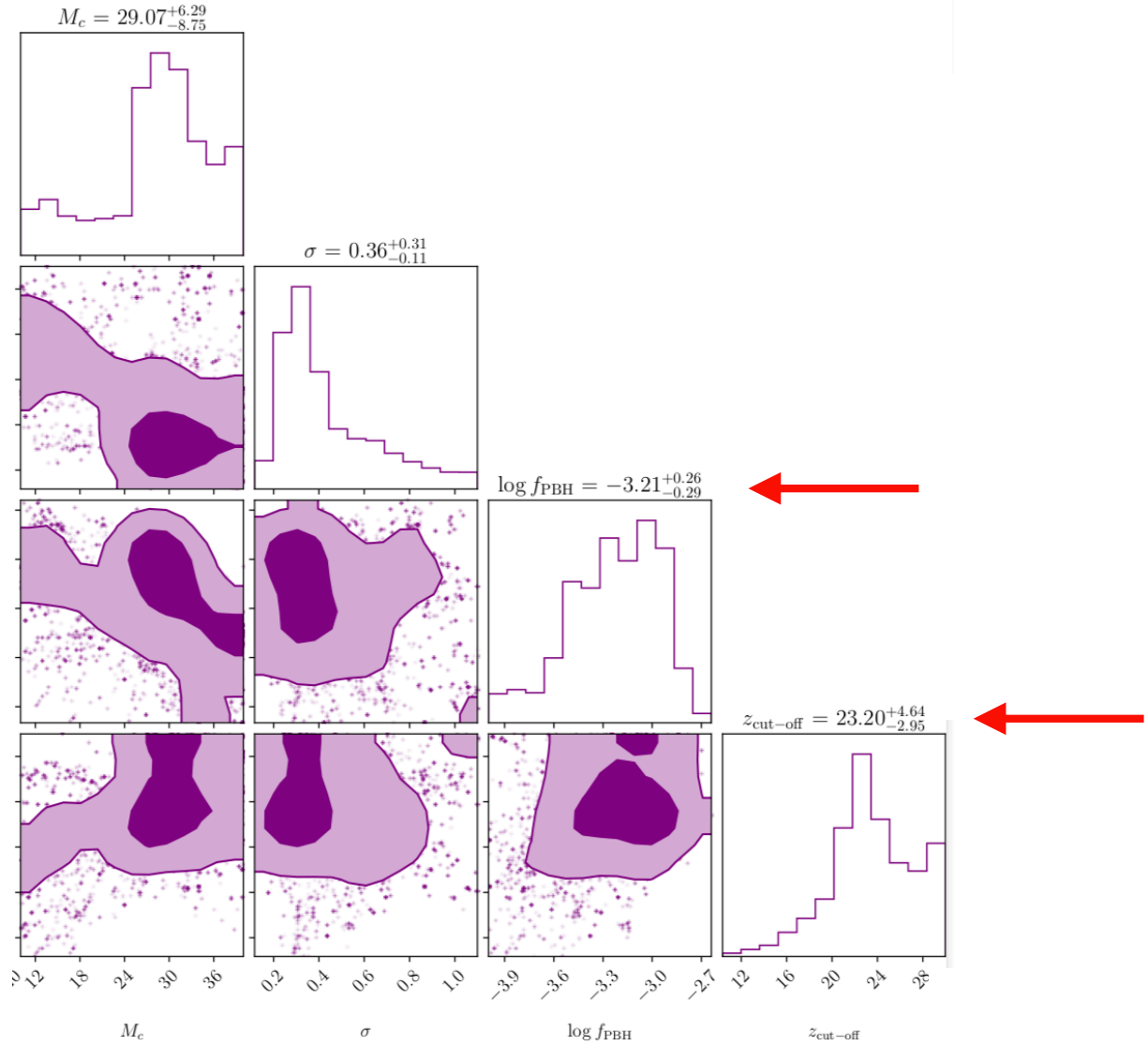

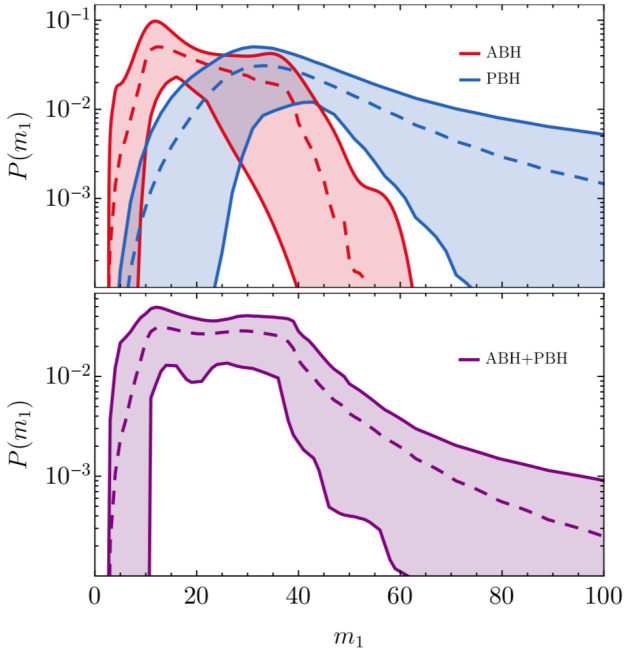

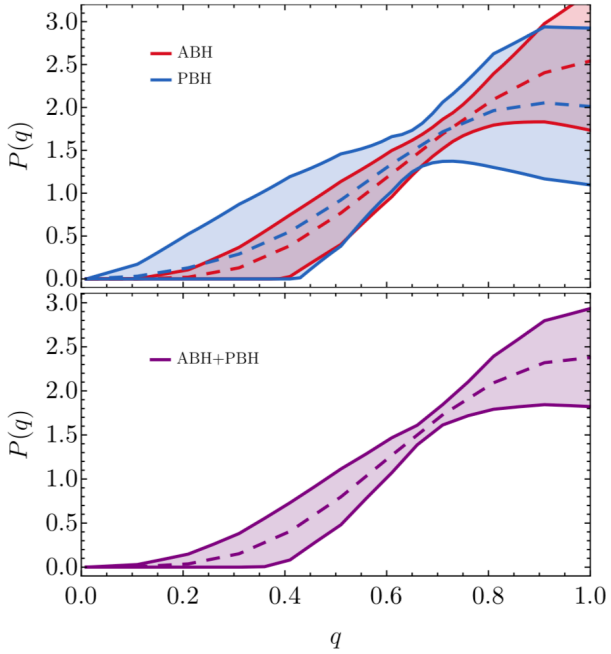

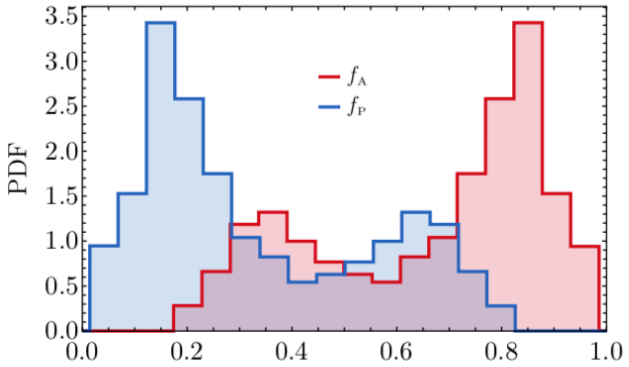

- ABH events account for roughly four times the PBH events
- Massive events accounted for by PBHs

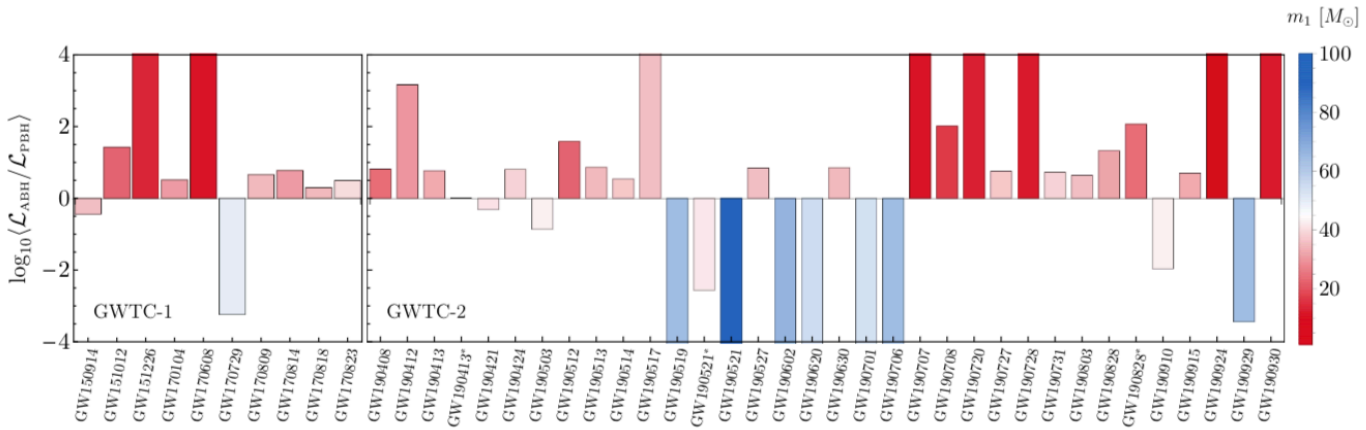

De Luca et al. (2021)

Statistical evidence

De Luca et al. (2021)

$$Z_{\mathcal{M}} \equiv \int \mathrm{d}\vec{\lambda}\, p(\vec{\lambda}|\vec{d})$$

$$\mathcal{B}^{\mathcal{M}_1}_{\mathcal{M}_2} \equiv \frac{Z_{\mathcal{M}_1}}{Z_{\mathcal{M}_2}} > (10, 10^{1.5}, 10^2) \Rightarrow \text{(strong, very strong, decisive evidence)}$$

$$\log_{10} \mathcal{B}^{\mathcal{M}}_{\mathrm{PBH+ABH}} \equiv \log_{10} \left(Z_{\mathcal{M}}/Z_{\mathrm{PBH+ABH}}\right)$$

PBH: - 4.91 ABH: - 2.17 PBH + ABH: 0

(Truncated/Power law + peak = - 2.1)

PBH constraints in the LIGO/Virgo mass range

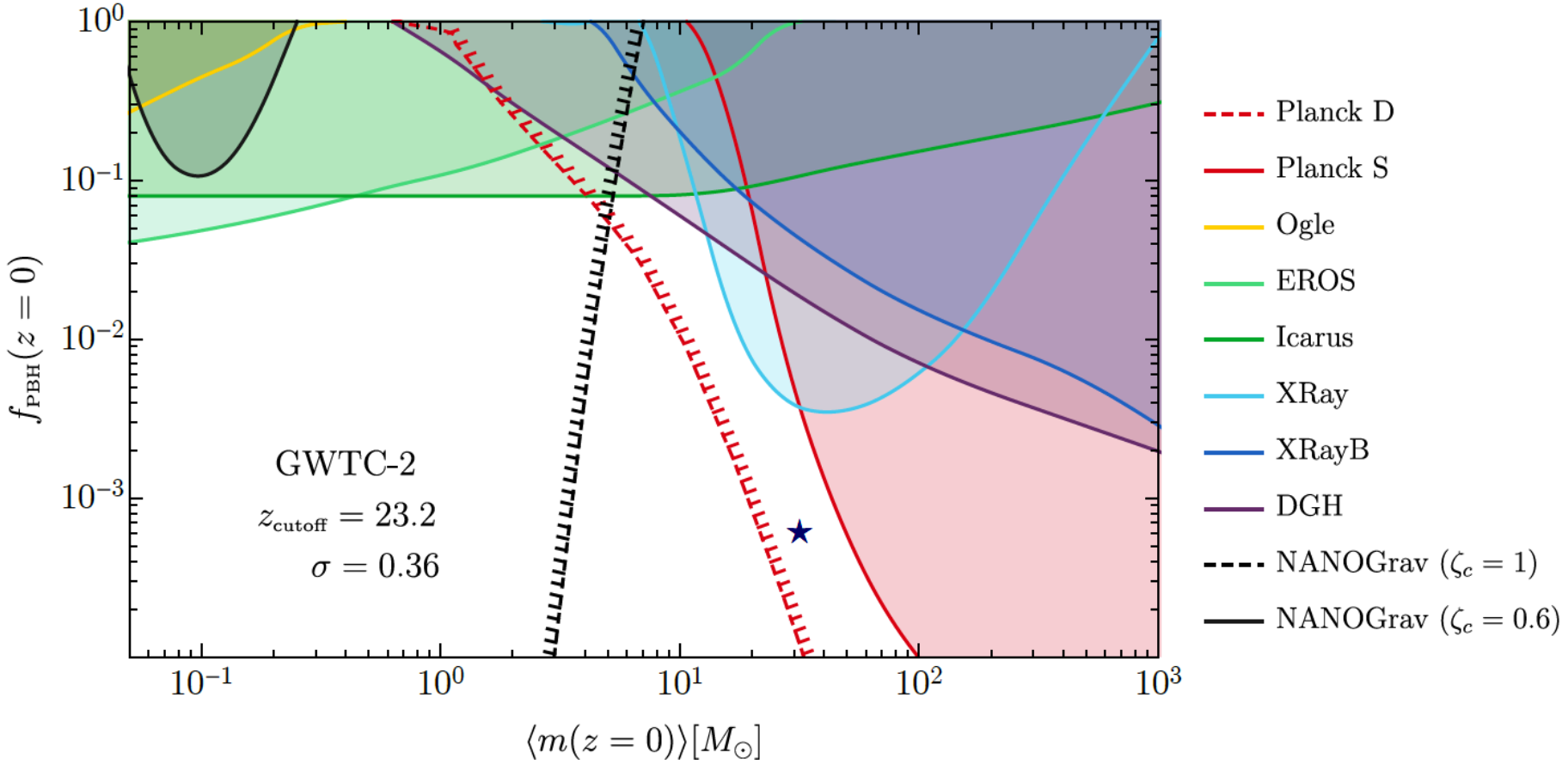

De Luca et al. (2021)

Mapping the GWTC-2 catalog into 3G detectors

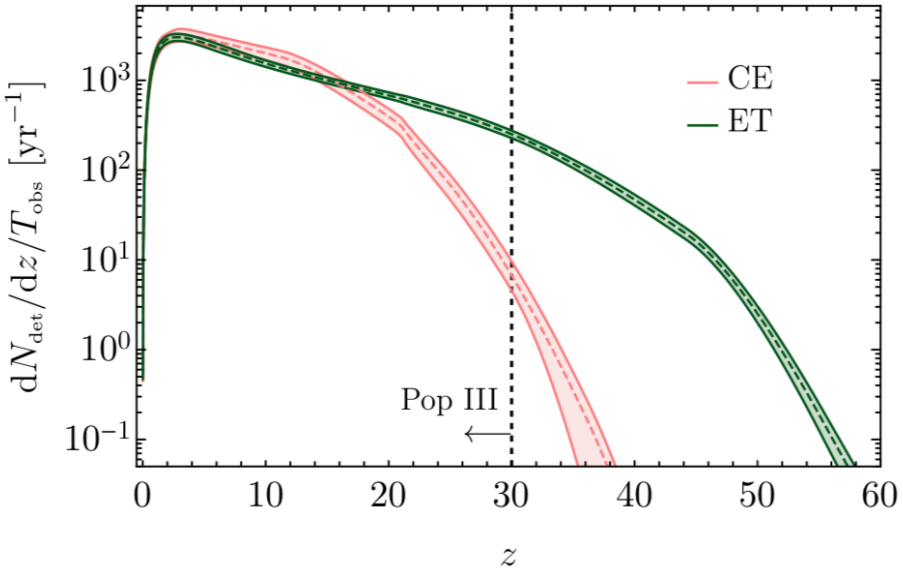

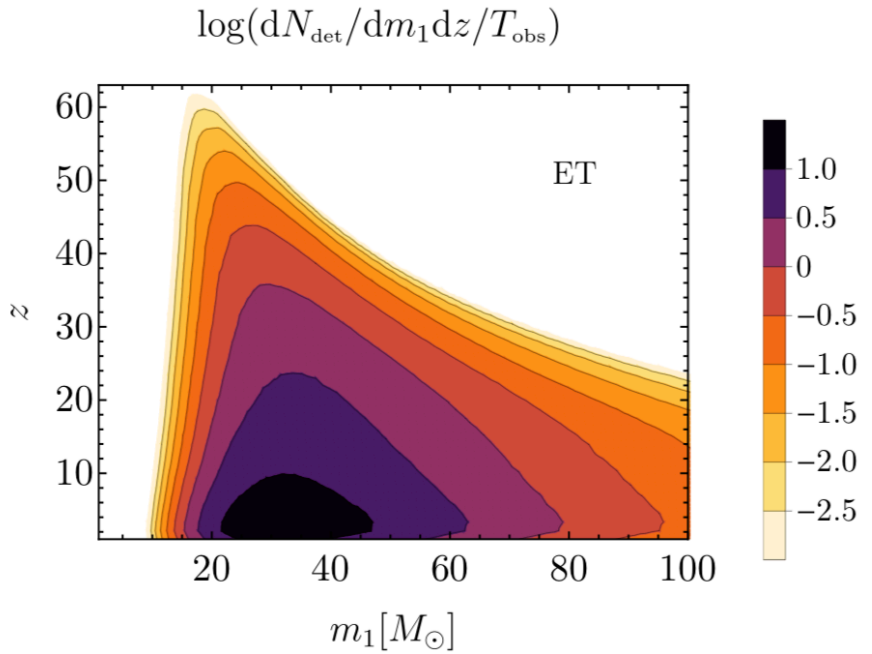

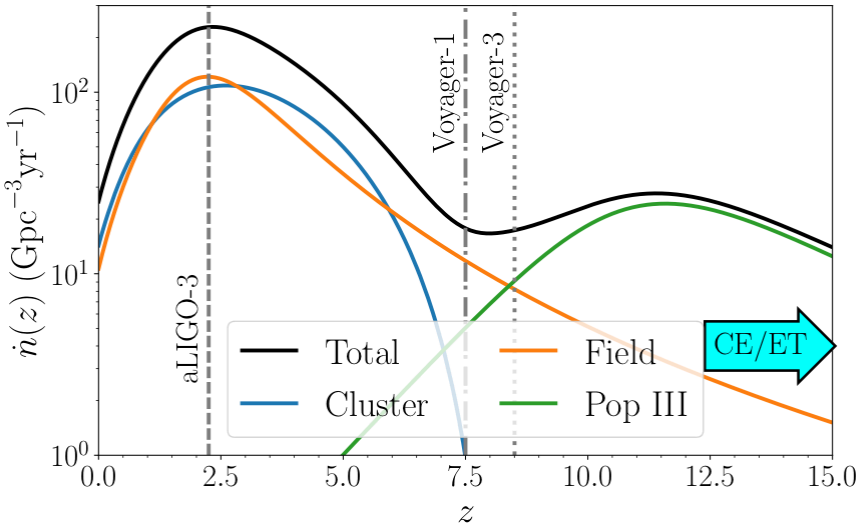

V. De Luca et al. (2021)

$$\frac{\mathrm{d}R_{\mathrm{PBH}}}{\mathrm{d}z} \sim t^{-34/37}(z)$$

Ng et al. (2021)

- GWTC-2 events may have a component of PBHs
- PBHs are not the dark matter in the LIGO/Virgo mass band
- 3G detectors will help to answer the question about the nature of the BHs in the LIGO/Virgo mass range

PBHs and the stochastic background of GWs

GWs from PBHs

The same curvature perturbations giving rise to PBHs are unavoidably a source for GWs at *second-order* in perturbation theory

$$\frac{\delta\rho}{\bar{\rho}} \sim \frac{\nabla^2\zeta}{a^2H^2}$$

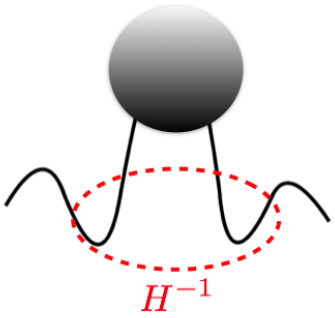

$$h''_{ij} + 2\mathcal{H}h'_{ij} - \nabla^2 h_{ij} = \mathcal{O}(\partial_i\zeta\partial_j\zeta)$$

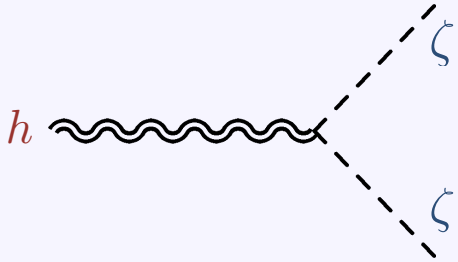

Potentially observable at current and future GW observatories

GW Power Spectrum

Power spectrum of GWs:

$$\left\langle h^{\lambda_1}(\eta,\vec{k}_1)h^{\lambda_2}(\eta,\vec{k}_2)\right\rangle' \approx \mathcal{P}_\zeta\mathcal{P}_\zeta$$

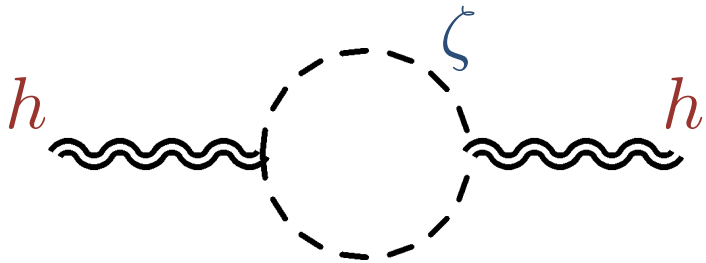

At second order in comoving curvature perturbation, after averaging over the fast oscillating pieces

$$\Omega_{\rm GW}(\eta,k) = \frac{\pi^2}{243\mathcal{H}^2\eta^2}\int\frac{d^3p}{(2\pi)^3}\frac{p^4\left[1-\mu^2\right]^2}{p^3\left|\vec{k}-\vec{p}\right|^3}\mathcal{P}_\zeta(p)\,\mathcal{P}_\zeta\left(\left|\vec{k}-\vec{p}\right|\right)\mathcal{I}^2\left(\vec{k},\vec{p}\right)$$

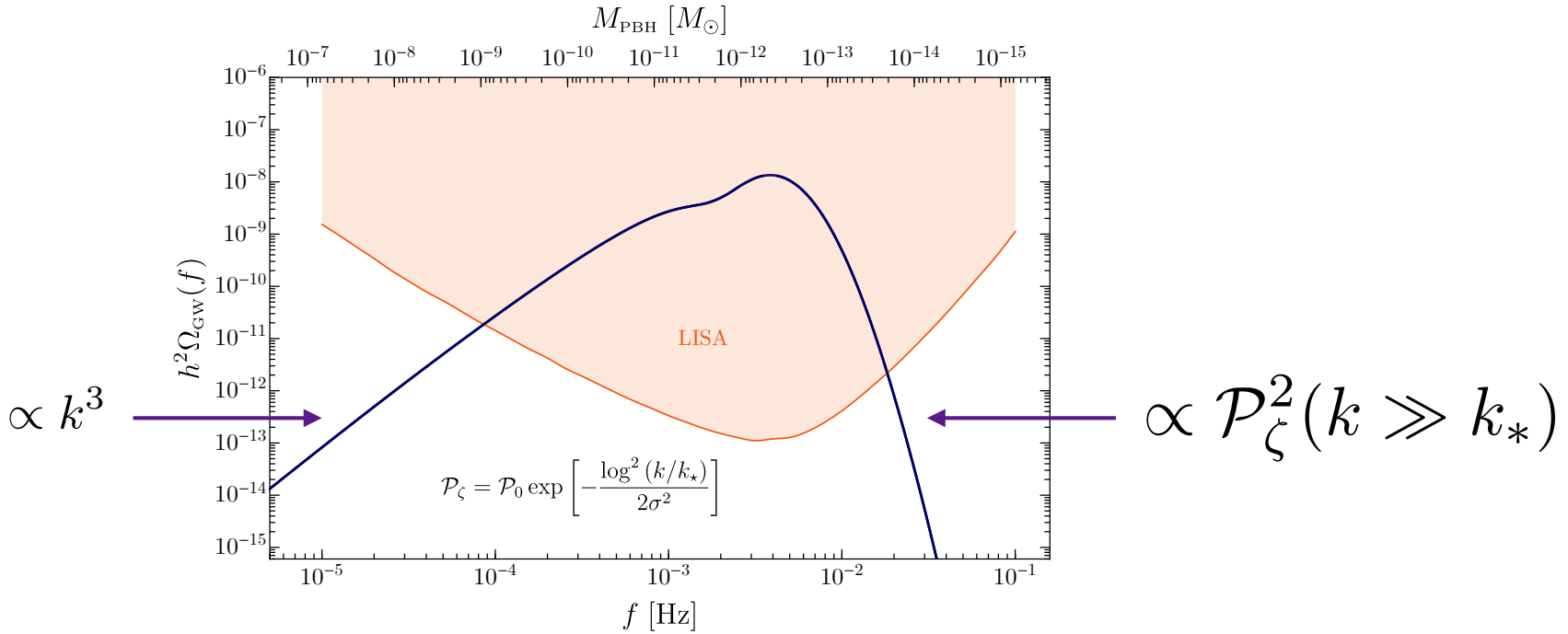

$\propto k^3$

$\propto \mathcal{P}_\zeta^2(k \gg k_*)$

The PBH dark matter-LISA serendipity

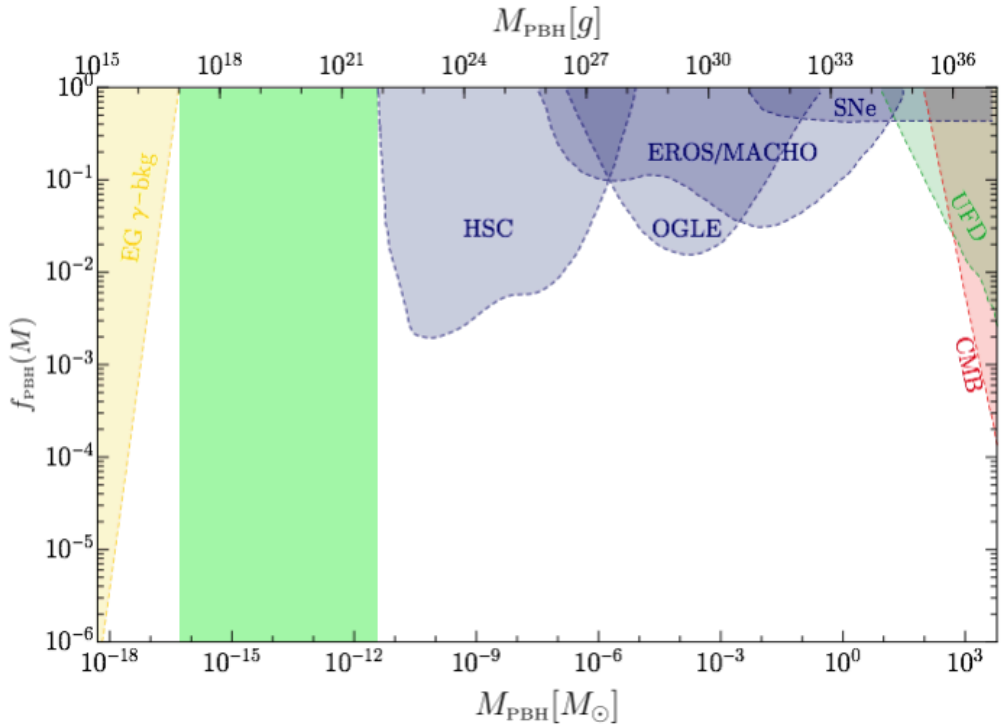

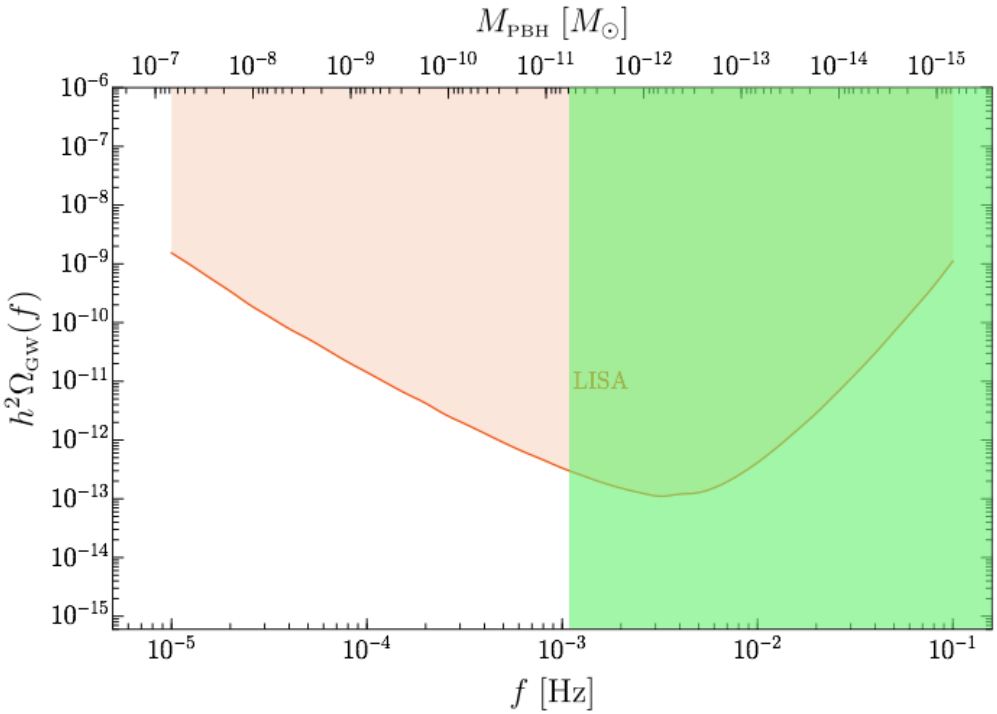

$$M \simeq 10^{-12} M_\odot \left(\frac{f_{\rm LISA}}{f}\right)^2$$

$$f_{\rm LISA} = 3.4 \text{ mHz}$$

$$M \approx 10^{-12} M_\odot$$

Bartolo et al. PRL (2019)

Nano-Grav 12.5 year

Millisecond pulsars whose signal sensitive to the stochastic GW background

Cross-correlation of timing residuals

$$S_{ab} = \Gamma_{ab} \frac{h_c^2}{12\pi^2 f^3}$$

Nano-Grav 12.5 year

Strong evidence for a stochastic common process across 45 pulsars

$$\Omega(f) = \frac{2\pi^2}{3H_0^2} A^2 f_{\rm yr}^2 \left(\frac{f}{f_{\rm yr}}\right)^{5-\gamma}$$

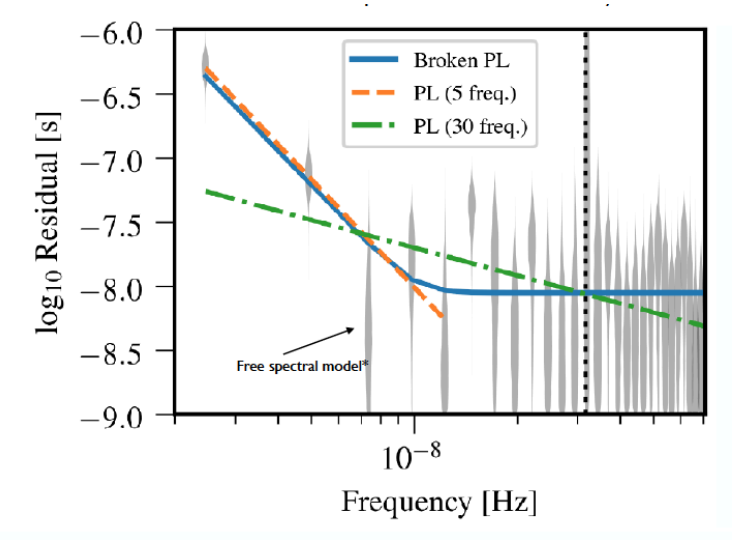

Possible flat spectrum with amplitude $\Omega(f) \sim 5 \cdot 10^{-10}$

Nano-Grav 12.5 year

Strong evidence for a stochastic common process across 45 pulsars

$$\Omega(f) = \frac{2\pi^2}{3H_0^2} A^2 f_{\rm yr}^2 \left(\frac{f}{f_{\rm yr}}\right)^{5-\gamma}$$

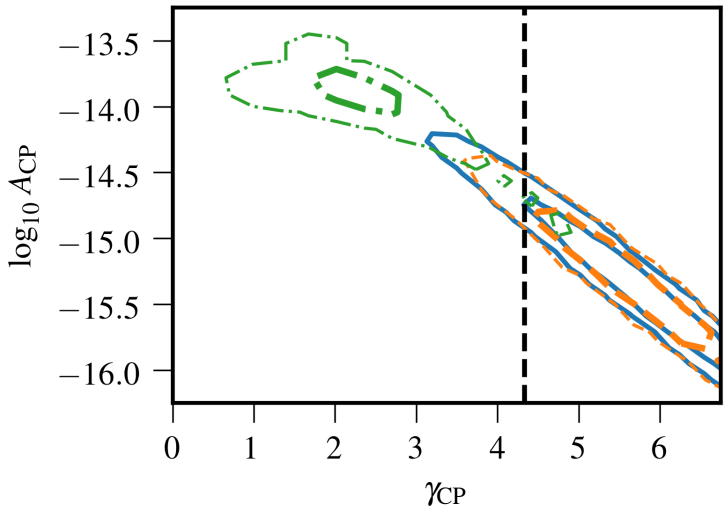

Possible flat spectrum with amplitude $\Omega(f) \sim 5 \cdot 10^{-10}$

Nano-Grav 12.5 year

Non-conclusive evidence for quadrupolar
Hellings-Downs (HD) correlation pattern (GW footprint)

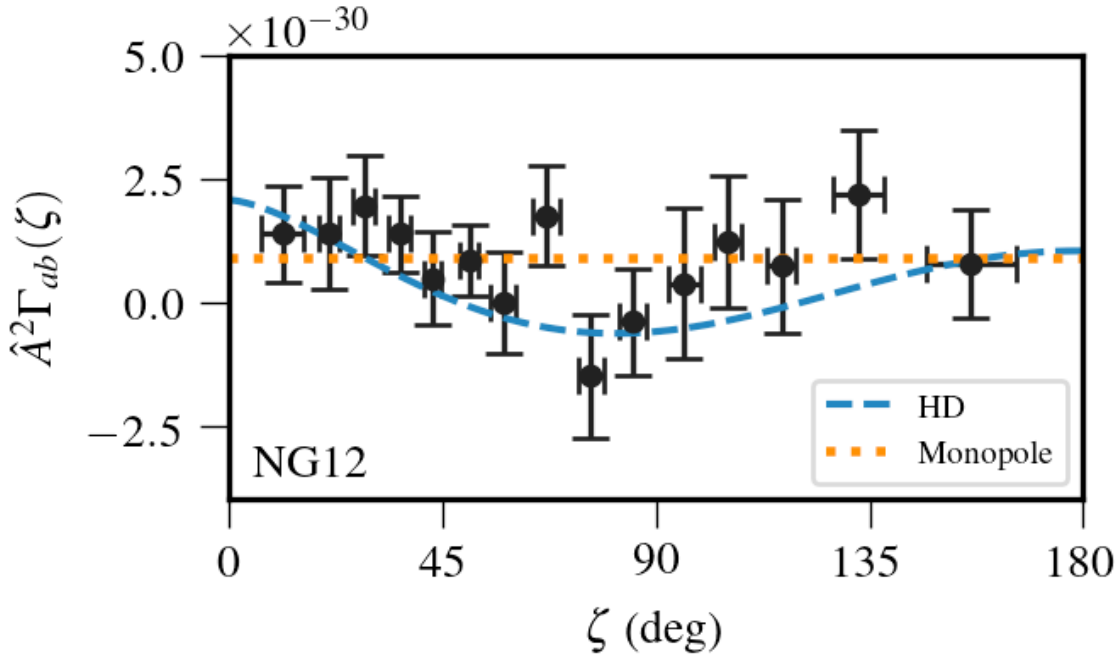

Need to wait for more data (two years on)

Can be consistent with a PBH = DM scenario

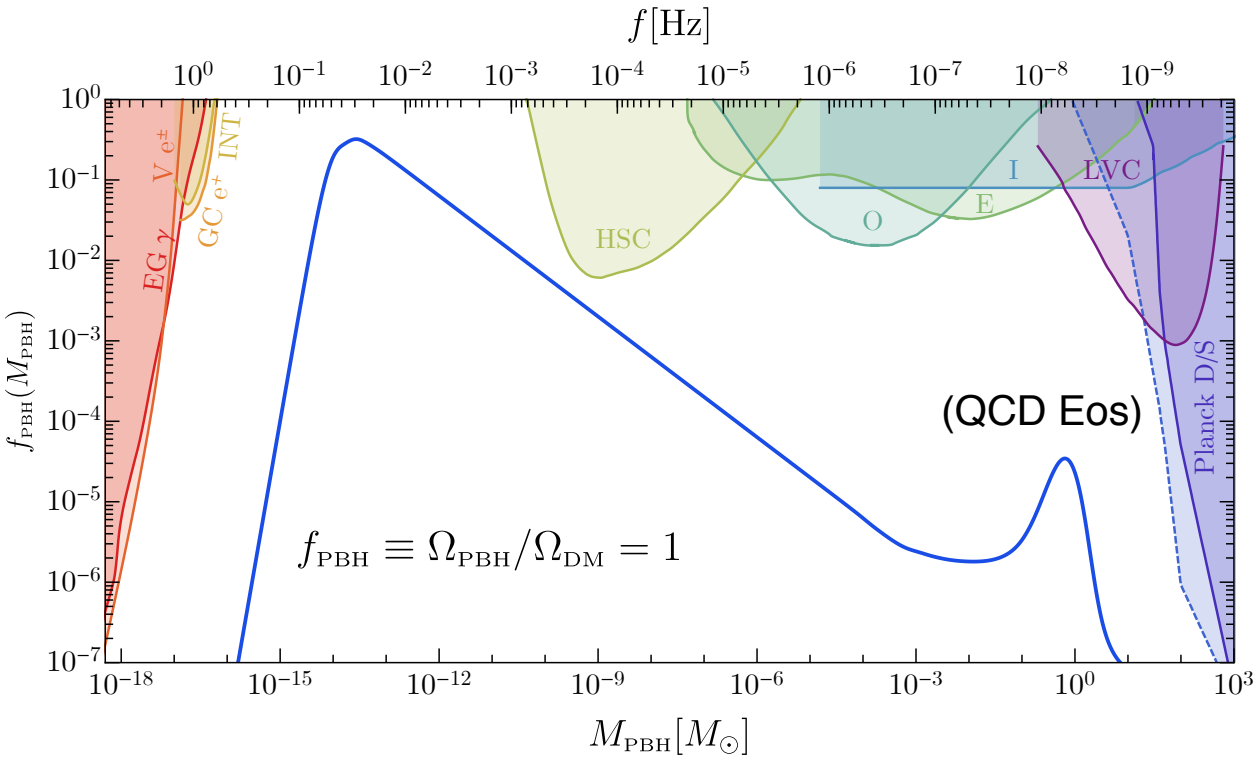

From flat curvature power spectrum

$$\mathcal{P}_\zeta(k) = A_\zeta \Theta(k_s - k)\Theta(k - k_l) \quad k_s \gg k_l$$

De Luca et al. PRL (2021)

Can be consistent with a PBH = DM scenario

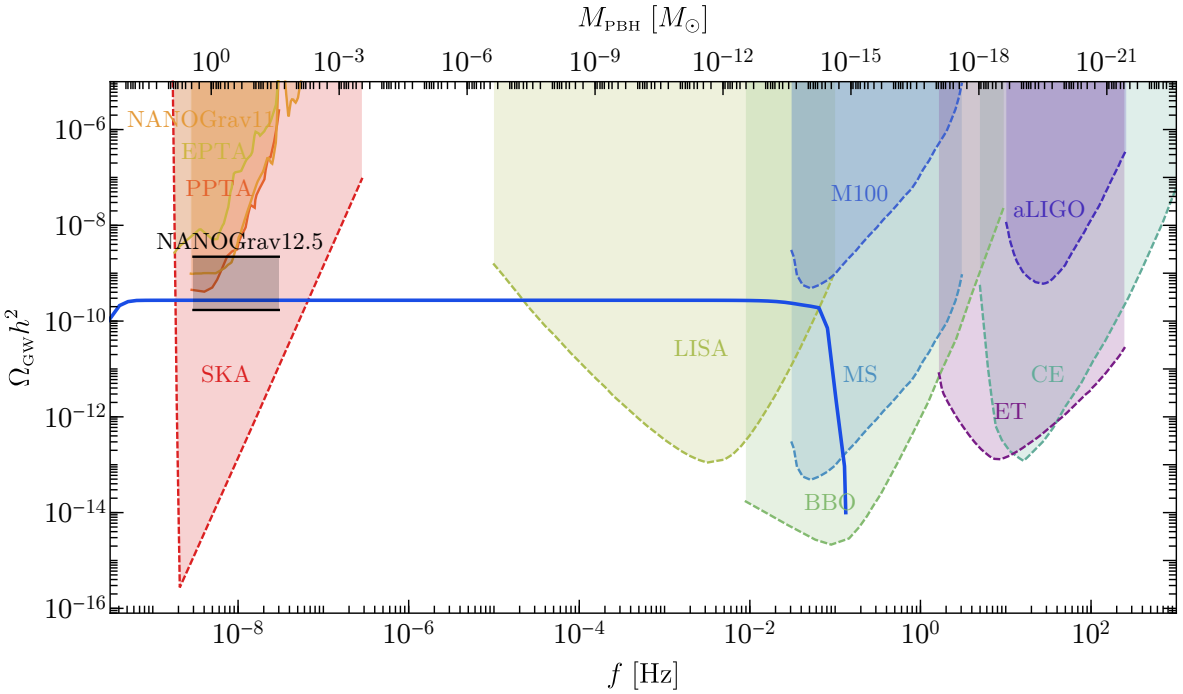

May be confirmed by LISA

Can be consistent with the HSC event

Hyper-Supreme Camera searches for microlensing of light from the Andromeda galaxy (M31)

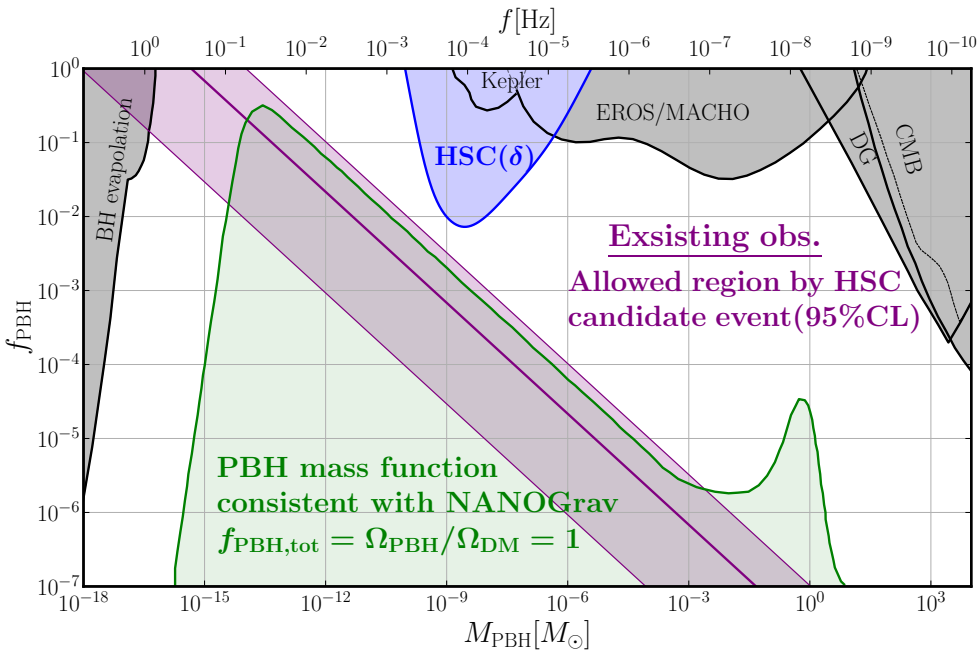

Allowed region allowed assuming a power-law mass function

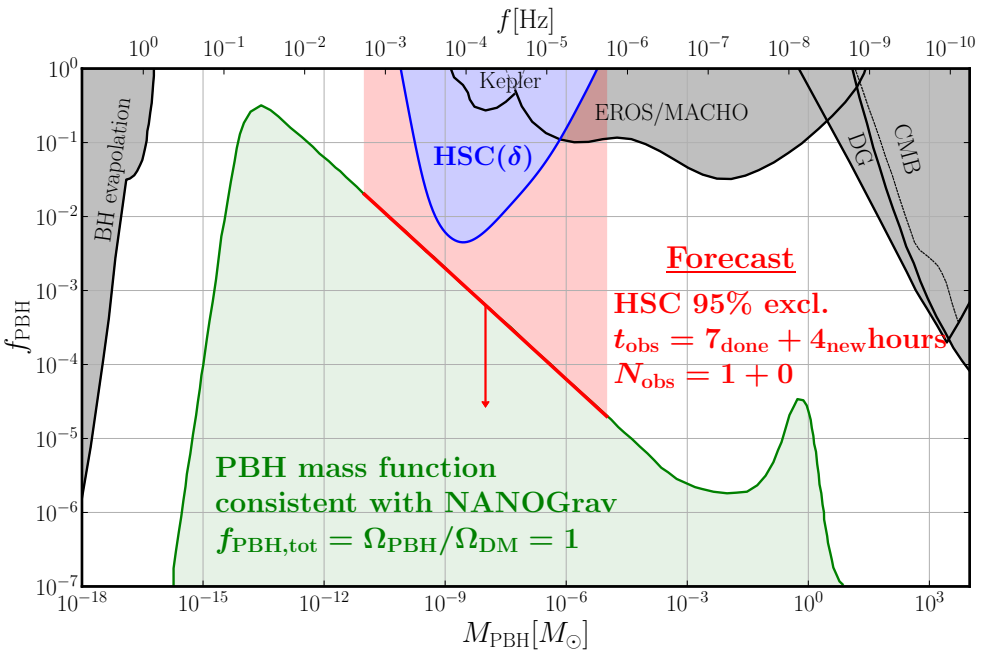

Forecast with longer observation time assuming null detection

Sugiyama et al. (2020)

Conclusions

- GWTC-2 events best fitted by ABH + PBH, not a surprise, PBHs are not the dark matter if in the LIGO/Virgo range, 3G detectors will have a say about the nature of BHs in the LIGO/Virgo mass range

- NANOGrav 12.5 yr signal consistent with the PBH scenario. If so, PBHs may comprise the totality of the dark matter